J Nanopart Res (2020) 22:117
https://doi.org/10.1007/s11051-020-04817-7

REVIEW

Nanotechnological solutions for controlling transmission and emergence of antimicrobial-resistant bacteria, future prospects, and challenges: a systematic review

Kenneth Ssekatawa · Dennis K. Byarugaba · Charles D. Kato · Francis Ejobi · Robert Tweyongyere · Michael Lubwama · John Baptist Kirabira · Eddie M. Wampande

Received: 16 October 2019 / Accepted: 12 March 2020

Abstract Globally, a high prevalence of multi-drug-resistant (MDR) bacteria, mostly methicillin-resistant *Staphylococcus aureus* and carbapenem-resistant *Enterobacteriaceae*, has been reported. Infections caused by such bacteria are expensive and hard to treat due to reduced efficient treatment alternatives. Centered on the current rate of antibiotics production and approvals, it is anticipated that by 2050 up to 10 million people could die annually due to MDR pathogens. To this effect, alternative strategies such as the use of nanotechnology to formulate nanobactericidal agents are being explored. This systematic review addresses the recent approaches, future prospects, and challenges of nanotechnological solutions for controlling transmission and emergence of

This article is part of the topical collection: Nanotechnology Convergence in Africa

Guest Editors: Mamadou Diallo, Abdessattar Abdelkefi, and Bhekie Mamba

K. Ssekatawa · D. K. Byarugaba · C. D. Kato · F. Ejobi · R. Tweyongyere · E. M. Wampande (✉)
College of Veterinary Medicine Animal Resources and Biosecurity, Makerere University, P. O. Box 7062, Kampala, Uganda
e-mail: ewampande@yahoo.co.uk

K. Ssekatawa
e-mail: Kssekatee@gmail.com

D. K. Byarugaba
e-mail: dkb@covab.mak.ac.ug

C. D. Kato
e-mail: katodrago@gmail.com

F. Ejobi
e-mail: ejobifrancis@gmail.com

R. Tweyongyere
e-mail: tmrobert966@gmail.com

K. Ssekatawa
Department of Biochemistry, Faculty of Biomedical Sciences, Kampala International University-Western Campus, P. O. Box 71, Bushenyi, Uganda

M. Lubwama · J. B. Kirabira
African Center of Excellence in Materials, Product Development and Nanotechnology: College of Engineering, Design, Art and Technology, Makerere University, P. O. Box 7062, Kampala, Uganda
e-mail: mlubwama@cedat.mak.ac.ug
e-mail: michaellubwama@gmail.com

J. B. Kirabira
e-mail: jbkirabira@cedat.mak.ac.ug

Published online: 12 May 2020

antibiotic resistance. A comprehensive literature search of PubMed and BioMed Central databases from June 2018 to January 2019 was performed. The search keywords used were "use of nanotechnology to control antibiotic resistance" to extract articles published only in English encompassing all research papers regardless of the year of publication. PubMed and BioMed Central databases literature exploration generated 166 articles of which 49 full-text research articles met the inclusion guidelines. Of the included articles, 44.9%, 30.6%, and 24.5% reported the use of inorganic, hybrid, and organic nanoparticles, respectively, as bactericidal agents or carriers/enhancers of bactericidal agents. Owing to the ever-increasing prevalence of antimicrobial resistance to old and newly synthesized drugs, alternative approaches such as nanotechnology are highly commendable. This is supported by in vitro, ex vivo, and in vivo studies assessed in this review as they reported high bactericide efficacies of organic, inorganic, and hybrid nanoparticles.

Keywords Multidrug resistance · Inorganic nanoparticles · Organic nanoparticles · Nanohybrid · Nanocarriers · Cytotoxicity · Nanomedicine

Background

The prevalence of nosocomial and community-acquired multidrug-resistant (MDR) bacterial infections with limited effective treatment options is on the rise worldwide (CDC 2013; CDDEP 2015). Notable examples include the increase in the incidence of methicillin-resistant *Staphylococcus aureus* (MRSA), emergence of MRSA clinical isolates insensitive to vancomycin (CDC 2013; Iyamba et al. 2014; Thati et al. 2011; Loomba et al. 2010), and high prevalence of carbapenem-resistant *Enterobacteriaceae* (CRE) infections. This is worsened by the fact that most of these resistant infections have no commendable treatment alternatives (Livermore et al. 2011; Nordmann et al. 2011, 2012). With such consequences, antimicrobial resistance (AMR) has resulted into increased morbidity and mortality to would-be unthreatening bacterial infections. Therefore, AMR has emerged as one of the leading threats to human and animal health (CDC 2013; Lowy 2003). A number of factors have been implicated as drivers of AMR. The most common ones include biofilms, overuse of antibiotics, irrational prescription of antibiotics, and the use of antibiotics in livestock to promote growth (Hausner and Wuertz 1999; Høiby et al. 2010; Economou and Gousia 2015; Warnes et al. 2012; Ceri et al. 1999). Overconsumption of antibiotics presents selective pressures to bacterial population where some adapt by developing molecular resistance mechanisms such as antibiotic resistance-encoding genes (Queenan and Bush 2007: Brody et al. 2008; Punina et al. 2015; Perez et al. 2007; Gulmez et al. 2008; Pfeifer et al. 2012; Poirel and Nordmann 2006; Perez et al. 2007), hence evolving to form resistant strains. A number of studies have documented the molecular mechanisms of AMR; these are summarized in Table 1 and Figs. 1 and 2.

Furthermore, leading pharmaceutical companies have shut down their antibiotics research and development programs due to the fact that antibiotics are less lucrative than other drugs used in the treatment of protracted ailments. This is mainly because (a) most new antibiotic generations are inaccessible, prohibited, shelved and used as last resort antibiotics ostensibly to protect them against resistance, and (b) they are used for a short period of time, and they become obsolete due to emergence of resistance limiting the initial return on investment (Nature Biotechnology Volume 36 Number 7 July 2018; Spellberg et al. 2004; Power and Schering–Plough Corporation 2006). Therefore, based on the present rate of antibiotic production and approvals, it is projected that by 2050, up to 10 million people could die annually due to MDR superbug infections (Nature Biotechnology Volume 36 Number 7 July 2018). Thus, this necessitates development of novel alternatives to antibiotics.

One of the promising strategies to control antibiotic resistance is the use of nanoparticle (NP) therapeutics, nanostructured coating of indwelling and other medical devices in addition to nanodrug delivery systems. Nanoparticles are materials where at least one dimension lies between 1 and 100 nm (Khan et al. 2017). Nanoscale materials have garnered attention since they occupy very little space but with a very large surface area to volume. Reducing material to nanoscale increases the surface area to volume ratio, and this affords the resultant NPs very high versatility, solubility, chemical reactivity, and different morphologies with different mechanisms of action (Padmavathy and Vijayaraghavan 2008; Simon-Deckers et al. 2009). Various types of NPs presently accessible and under fabrication include inorganic metals, organic polymers, organic natural compounds, and nanostructured materials. Diverse engineering

Table 1 Molecular mechanisms of antibiotic resistance

Type of antibiotic resistance	Molecular mechanism of resistance	Reference
Limiting entry of antibiotics	Mutation in the gene-encoding outer membrane porin (OMP) protein through which antibiotics diffuse into the cell resulting into altered OMPK36 variant porin with reduced permeability to antibiotics in *K. pneumoniae*	Nordmann et al. 2012
	Decreased permeability to antibiotics in *E. coli, Pseudomonas* spp., and *Acinetobacter* due to downregulation of the main porins or replenishing the cell membrane with novel selective protein channels	Lavigne et al. 2013; Tangden et al. 2013; Novais et al. 2012
Acquisition of multiple chromosomal and plasmid efflux pump genes	Efflux pumps actively drive several antimicrobials out of the cell. Their upregulation provides resistance to previously clinically efficacious antibiotics, such as broad-spectrum MDR efflux pumps in *E. coli* (AcrB) and *P. aeruginosa* (MexB)	Ruggerone et al. 2013; Hinchliffe et al. 2013
Modification and protection of antibiotics target	Change the configuration of the targets, thereby reducing the binding affinity of antibiotics. *K. pneumoniae* and *S. aureus* resistance to linezolid were achieved through modifications in alleles encoding 23S rRNA ribosomal subunit in Gram-positive bacteria linezolid target	Billal et al. 2011; Gao et al. 2010
	Resistance to macrolides, lincosamines, and streptogramins through methylation of their binding site, the 16S rRNA by the erythromycin ribosome methylase (erm) family genes. Resistance to phenicols, pleuromutilins, streptogramins, lincosamides, and oxazolidonones, mediated by the addition of a methyl group to A2503 in the 23S rRNA by enzyme chloramphenicol-florfenicol resistance (cfr) methyltransferase	Long et al. 2006
	Methicillin resistance in *Staphylococcus aureus* due to the acquisition of the chromosomal mecA gene that transcribes for a single supplementary penicillin-binding protein, PBP2a with low affinity for all β-lactams	Stapleton and Taylor 2002, Neu 1992; Spratt 1994
Hydrolytic enzyme-mediated antibiotic resistance	Main molecular mechanism of resistance is through acquisition of chromosomal and plasmid-borne gene encoding for antibiotics degrading enzymes. Notable example is of β-lactamases which include penicillinases which degrade only penicillins, cephalosporinases which favorably deactivate cephalosporins and aminopenicillins, extended-spectrum β-lactamases (ESBL) that digest all β-lactams but carbapenems and carbapenemases that incapacitate all β-lactams	Ssekatawa et al. 2018; Nordmann et al. 2012
Modification of antibiotic-mediated resistance	Acquisition of genes coding for enzymes that inactivation of antibiotics via addition of functional group. Aminoglycolides resistance in *Campylobacter coli* is due to acetylation, phosphorylation, and nucleotidylation of its hydroxyl and amide exposed groups by acetyltransferases, phosphotransferases, and nucleotidyltransferases	Wright 2005

systems are required to fabricate these nanoparticle types, and each type can exhibit a variety of biomedical functions via different modes of action. NPs have demonstrated potent antibacterial activity in ex vivo, in vivo, and in vitro experiments. Thus, these NPs have attracted the attention in the health sector to be used as alternative or co-antimicrobial agents, nanoantibiotics delivery systems, and nanostructured coatings owing to their undisputed bactericide ability mediated by different mechanisms (Simon-Deckers et al. 2009).

Inorganic metal NPs such as silver, gold, zinc, copper, and titanium and organic NPs such as chitosan have been experimented as substitutes to antibiotics and conventional disinfectants. Notable examples include the use of NPs to avert catheter-associated infections and biofilm formation and the use of NPs in antimicrobial wound dressing and coatings (Padmavathy and Vijayaraghavan 2008; Simon-Deckers et al. 2009; Li et al. 2011; Ren et al. 2009; Meghana et al. 2015; Lai et al. 2015; Jahnke et al. 2016; Shahverdi et al. 2007;

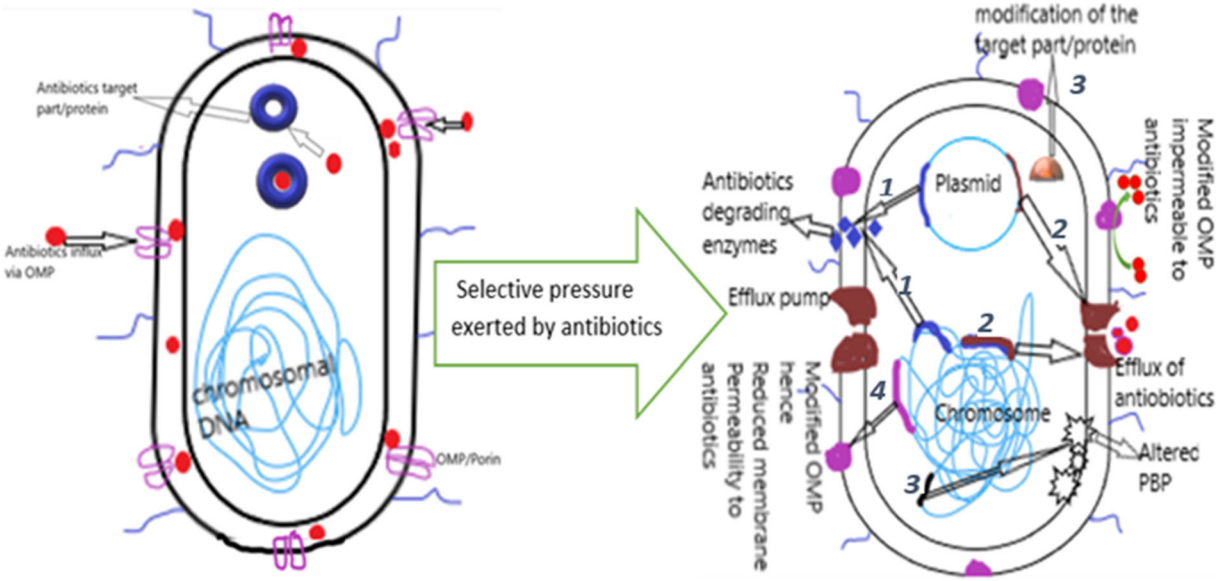

Fig. 1 Molecular mechanisms of antibiotic resistance. (Addae et al. 2014) Acquisition of chromosomal and plasmid antibiotics resistance genes (gene-encoding enzymes which (a) hydrolyze antibiotics and (b) modify drugs). (Ali et al. 2011) Acquisition of antibiotics efflux pump genes. (Alves et al. 2017) Mutation in the gene encoding a vital target protein such (PBP) so that an altered drug target is expressed. (Ansari et al. 2014) Mutation in gene expressing OMP so that a truncated OMP is produced or there is downregulation of OMP

Ivask et al. 2014; 35. Pérez-Díaz et al. 2015; Cui et al. 2013; Ramalingam et al. 2016; McQuillan and Shaw 2014; Ali et al. 2011). However, the emergence of resistance to Ag NPs and other heavy metals in *Escherichia coli* threatens the use of metal NPs as substitutes to antibiotics (Panáček et al. 2017; Tajkarimi et al. 2017). This resistance is attributed to the (a) acquisition and upregulation of efflux pumps for Ag NPs and other metal nanomaterials; (b) enzymatic alterations of nanomaterials such as oxidation, reduction, methylation, and demethylation; (c) gaining and overexpression of metal-binding proteins notably metallothionein, SmtA, chaperone CopZ, and SilE (Silver and Phoung 2005); (d) limiting entry of nanomaterials by mutation and suppression of expression of genes encoding the metal ion transmembrane proteins (Graves et al. 2015); and (e) extracellular secretion of flagellin adhesive protein that induce agglomeration of silver NPs (Tajkarimi et al. 2017). To achieve meaningful outcomes, attempts should be made to design nanotherapeutic agents with the capacity to circumvent the modes of resistance to heavy ionic and nanoscale metals in addition to the molecular mechanisms of resistance that have rendered conventional antibiotics obsolete. Therefore, the fabrication process of antibacterial nanomaterial should encompass strategies to overcome the emergence of resistance to the novel nanotherapeutic agents as well as shielding antibiotics from the various mechanisms of resistance.

Pathogen acquisition of AMR to a single therapeutic agent is not complex as resistance can be achieved through relatively simple genomic modifications (Fig. 2) (Tajkarimi et al. 2017). Therefore, antimicrobial combinatory strategy is the most promising approach to curb antimicrobial resistance (Asgarali et al. 2009). This may entail fabrication of nanocomposites through combination of antibiotics and nanomolecules with antibacterial activity, two or three nanosubstances, and loading antibiotics and NPs in nanodrug delivery systems (Fig. 2). Combinatory effects of NPs and antibiotics, two or more nanosubstances, will most likely evade bacterial antimicrobial resistance mechanisms, while nanodrug vehicles with antibacterial activity, such as silver NPs, copper NPs, chitosan NPs, among others, will not only protect antibiotics from the molecular mechanisms of resistance but will confer the nanodrug delivery system-antibiotics complex synergistic antibacterial effect; that is to say, conventional antibiotics will be re-potentiated by synergistic combination with NPs against MDR bacteria (Selvaraj et al. 2019). For

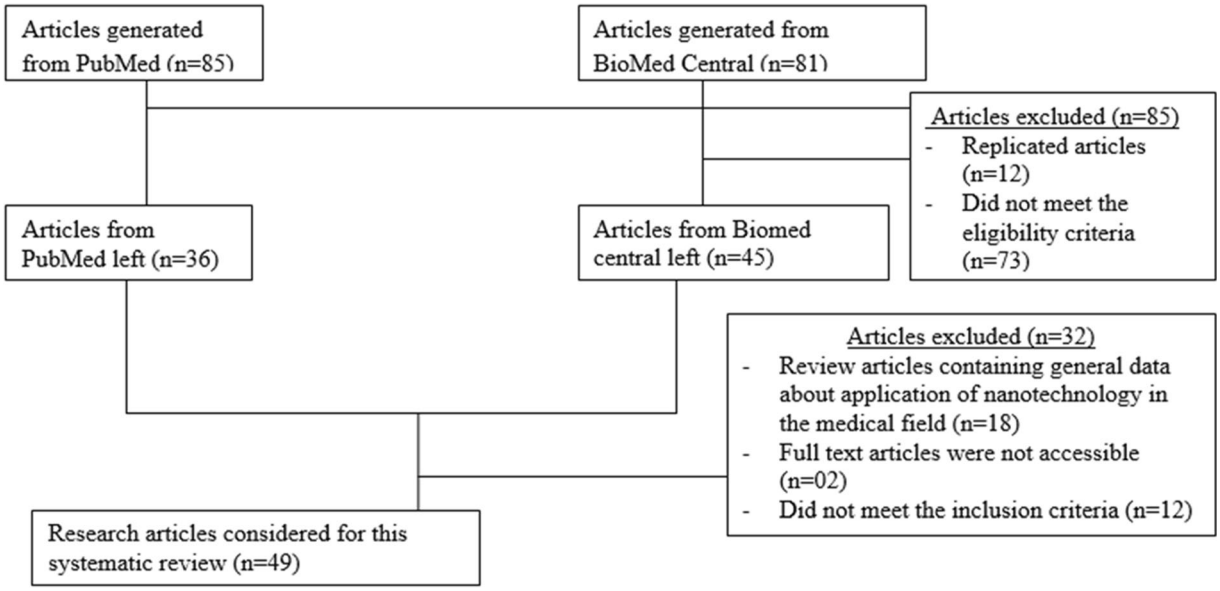

Fig. 3 Selection process of research articles for inclusion in this systematic review

fulfilled the inclusion guidelines for this systematic review (Fig. 3).

Inorganic nanoparticles

Out of the 49 articles included in this systematic review, 22 articles reported the use of nanoparticles generated from inorganic metal irons as antibacterial agents. Eight articles reported the use of silver NP (Umashankari et al. 2012; Palanisamy et al. 2014; Sowmya et al. 2018; Raman et al. 2017; Bansod et al. 2015; Rafińska et al. 2019; Reithofer et al. 2014; Singh et al. 2014); three articles reported use of titanium (Cheng et al. 2009; Senarathna et al. 2017; Ercan et al. 2011); and one article in each case reported the use of gold (Naz et al. 2013), zinc (Seil and Webster 2012), aluminum (Ansari et al. 2014), magnesium (He et al. 2016), cadmium (Salehi et al. 2014), and nanoshield (Michalikova et al. 2017). Two studies compared the antimicrobial activity of two metal nanomaterials independently, zinc and titanium (Khan et al. 2016) and gold and iron (Chatterjee et al. 2011). Other studies attempted to investigate the synergism of two metal NPs; one study in each case investigated the synergism of zinc and silver (Jafari et al. 2017), gold and copper (Addae et al. 2014), and gold and silver (Islam et al. 2017) NP cocktails (Table 2).

Inorganic-organic hybrid nanocomposites

Inorganic-organic nanohybrids are nanocomposites formed by conjugation of inorganic NPs to organic nanoscale or non-nanoscale polymers (de la Fuente and Grazu 2012). The literature search generated 15 research reports in which inorganic-organic nanohybrids were used. Eight studies reported the use of nanosilver-based polymers; thermoplastic polyurethane (TPU)-polydopamine (DA) silver nanopolymer (TPU-NS2.5) released silver ions with 100% antibacterial activity against *Pseudomonas aeruginosa*, *Escherichia coli*, *Staphylococcus aureus*, and methicillin-resistant *Staphylococcus aureus* (MRSA) in in vitro assay and protected 100% of mice from MRSA-induced wound infections in in vivo studies and TPU-DA possessed no antibacterial activity (Liu et al. 2018). The bacterial activity of pegylated silver-coated single-walled carbon nanotubes (pSWCNT-Ag) and silver-coated single-walled carbon nanotubes (SWCNT-Ag) was compared. Both nanocomposites exhibited potent antibacterial activity against *E. coli* at concentrations of 50 and 62.5 μg/ml. For *Salmonella enterica* serovar *typhimurium* and *Salmonella enterica* serovar *anatum*, only pSWCNT-Ag at 62.5 μg/ml had potent antibacterial activity. Furthermore, at a concentration of 50 μg/ml pSWCNT-Ag and both 50 and 62.5 μg/ml, non-pegylated SWCNT-Ag had partial to no growth suppression effects on *S. typhimurium* and *S. anatum* (Park et al.

2018). In another study, polyhydroxyethyl methacrylate (PHEMA) was loaded with silver NPs. The hydrogel released silver NPs efficiently with in vitro and in vivo efficacy of 100% against *E. coli* and *S. aureus* infections in mice (Xu et al. 2018). Silver NPs were adsorbed on silicate platelet to form a stabilizing nanocarrier for silver NPs with 100% bactericide effect on *E. coli*, *S. aureus*, and *S. typhimurium* (Su et al. 2011). In another study, bone morphogenetic protein 2 (BMP-2) coupled-nanosilver-poly-DL-lactic-co-glycolic acid (PLGA) composite grafts were designed. They demonstrated 100% efficacy against vancomycin-resistant MRSA in vitro and in vivo (mice) assays (Zhenga et al. 2010). Silver NP-doped calcium phosphate-based ceramic-coating titanium prosthetic implants rescued 89% (8 out of 9) rabbits, while the control (calcium phosphate-based ceramic-coating titanium prosthetic implants) rescued 11% (1 out of 9) of the rabbits from MRSA bone infections (Kose et al. 2013). Two studies reported the synergism of the compounds within a nanohybrid. In one study, silver NPs conjugated to curcumin exhibited a combinatory antimicrobial effect of 100% on *E. coli* and *P. aeruginosa* (Alves et al. 2017), while gold NPs' surface modified by polyelectrolyte (PAH) and silver NPs had a synergistic inhibitory effect of 100% on *E. coli* and *Bacillus Calmette-Guérin* (Zhou et al. 2012) (Table 3).

Regarding nanodrug delivery systems, two studies employed iron oxide NPs. Niemirowicz et al. (2015) designed a ceragenin-coated iron oxide magnetic NPs (MNP-CSA-13). Iron oxide magnetic NPs were used to deliver CSA-13 antimicrobial peptide. The CSA-13 exerted a 100% inhibitory activity of free-living and biofilm *P. aeruginosa* at a concentration of 10 μg/ml and 100 μg/ml, respectively. In the second study, Chemello et al. (2016) designed an iron oxide NPs-oxytetracyclin nanocarrier system. The nanodrug vector delivered the antibiotic effectively to the target zebrafish tissues infected with bacterial pathogens without exhibiting toxic effects to the host cells (Table 3).

One study in each case employed zinc, gold, bismuth, and cadmium-titanium NPs linked to other organic substances. Zinc oxide nanorods-graphene nanoplatelets (ZNGs) nanocomplex successfully eliminated 100% *S. aureus* and *P. aeruginosa* planktons and 96% and 50% of *S. aureus* and *P. aeruginosa* biofilms (Zanni et al. 2017). Anwar et al. (2018) functionalized pefloxacin using (dimethylamino) pyridine propylthioacetate-coated gold nanoparticles (DMAP-PTA). The latter and the former were inactive against *E. coli*. But after combining them, DMAP-PTA-pefloxacin nanohybrid achieved a bactericide effect of 100% on *E. coli*. Luo et al. (2013) used bismuth NPs as a vector to deliver polyclonal *P. aeruginosa* antibodies. The bismuth nanocarrier preserved the viability of the antibodies, and they exhibited antibacterial efficacy of 90% against MDR *P. aeruginosa* compared with 6% without the nanocarrier in vitro experiments. Cadmium tellurium (CdTe) and titanium oxide (TiO_2)-CdTe-TiO_2 nanocomposite capped with mercaptopropionic acid (MPA) and conjugated with semiconductor quantum dots (QDs) exhibited an antibacterial activity of 99.9% against *E. coli* and *B. subtilis* planktons and 60% against *P. aeruginosa* (Gholap et al. 2013). Inorganic-organic Ormostamp surfaces with nanopillar arrays fabricated using UV nanoreplication technology completely inhibited the growth of *S. aureus* (Wu et al. 2018) (Table 3).

Organic nanomolecules

The search yielded 12 articles reporting the use of nanoorganic molecules as antibacterial agents or antimicrobial nanocarriers. Nine studies investigated the use of nanoorganic compounds as drug delivery system. Nanoemulsions enclosing *Cymbopogon flexuosus* (Da Silva Gündel et al. 2018), solid lipid NPs loaded with *Eugenia caryophyllata* essential oil (SLN-EO) (Fazly Bazzaz et al. 2018), chitosan NP holding ciprofloxacin (Cipro/CSNPs) (Marei et al. 2018), methacrylate nanocarrier delivery system packaging clavanin A (Saude et al. 2014), oleic acid (OA)-monomethoxy polyethylene glycol (mPEG) nanocarrier loaded with vancomycin (Omolo et al. 2017), imipenem/cilastatin loaded poly Ɛ-caprolactone (PCL), and polylactide-*co*-glycolide (PLGA) nanocapsules (Shaaban et al. 2017) exhibited enhanced antibacterial activity against antibiotic-resistant and non-resistant clinical isolates. For instance, these nanodelivery systems enhanced the efficacy of imipenem and vancomycin to 74–78.4% and 86.8%–90.5% against imipenem-resistant isolates (*K. pneumoniae* and *P. aeruginosa*) and MRSA, respectively, while graphene oxide (GO) nanosheet carrier had no augmentation on bactericide effect of sulfamethoxazole (SMZ) (Zou et al. 2016). Two studies applied nanocarriers coated with pro-inflammatory molecules to promote cell-mediated immune response.

Table 2 Inorganic nanoparticles used as antibacterial agents and methods of fabrication and characterization

Nanomaterial	Preparation of nanoparticles	NP characterization methods and properties	Target organisms	Form of application	NP exposure time (hr)	NPs mechanism of action	Efficacy (%)	Effective dose (μg/mL)	Ref
Iron oxide and gold	Chemical co-precipitation of Fe^{2+} and Fe^{3+} ions in an alkaline solution and treatment under hydrothermal conditions HAuCl4 solution was reduced by 10 mM NaBH4 solution under stirring condition and additional reduction by 10 mg/ml solution of dextrose	TEM and DLS	*E. coli*	Antibacterial activity and vector for ampicillin resistance gene	8	–	100 for Fe 0 for Au	200	Chatterjee et al. (2011)
Gold NPs/copper sulfide	–	HRTEM	*B. anthracis*	Antibacterial activity	24	Membrane perforation as revealed by SEM imaging and imaging and energy dispersive X-ray spectroscopy (EDS)	100 for anthracis cells 17 for spores	4.15 μM = 1081 μg/-ml	Addae et al. (2014)
Titanium dioxide photocatalyst NPs	Sol-gel method	SEM and DLS	*S. Flexner*, *A. baumannii*, PDR *A. baumannii*, and *S. aureus*	Antibacterial activity	0.67	–	100	200 μg/ml	Cheng et al. (2009)
Magnesium oxide	Purchased from Nanostructured and Amorphous Materials, Inc. (Houston, TX, USA)	–	*Campylobacter jejuni*, *E. coli* O157:H7, and *Salmonella enteritidis*	Antibacterial activity	24	Cell membrane damage as revealed by SEM	100	8000 μg /ml	He et al. (2016)
Gold/silver	*Prunus domestica* gum-mediated biosynthesis	UV-vis, FTIR, SEM, EDX, and XRD techniques	*S. aureus*, *E. coli*, and *P. aeruginosa*	Antibacterial activity	24	–	100	5 μg/ml	Islam et al. (2017)
Gold	Biosynthesized by 2, 4-dihydroxybenzene carbodithioic acid, a reducing and stabilizing agent	TEM, FT-IR and UV-vis spectrophotometry Size: 10–30 nm	*E. coli*	Antibacterial activity	72	–	100	0.5 mg/ml 500 μg/ml	Naz et al. (2013)
Silver	Purchase from Sigma-Aldrich, Sdn Bhd, Malaysia	XRD Size: 20–30 nm	*P. aeruginosa* biofilms	Antibacterial activity	24		Antibiotics sensitive-67 MDR 56	20 μg/ml	Palanisamy et al. (2014)
Titanium oxide NPs	Purchase from Sigma-Aldrich and functionalized by *Garcinia zeylanica* extract	SEM, XRD, and ATR-FTIR Size: 21 nm	MRSA	Antibacterial activity	24	–	99.99	13.9 g/l = 13,-900 μg/ml	Senarathna et al. (2017)
Silver	Silver NPs biosynthesized by *Phyllanthus acidus*	TEM, XRD, FESEM, and EDX	*E. coli*	Antibacterial activity	18		100	20 and 40 μg/ml	Sowmya et al. (2018)

Table 2 (continued)

Nanomaterial	Preparation of nanoparticles	NP characterization methods and properties	Target organisms	Form of application	NP exposure time (hr)	NPs mechanism of action	Efficacy (%)	Effective dose (μg/mL)	Ref
		Zeta potential: − 16.4				Cell membrane damage as revealed by SEM			
Silver	Silver NPs biosynthesized by mangrove plant (*Rhizophora mucronata*) extract	UV-visible spectrophotometry, XRD, FTIR, and HRTEM Size: 4 to 26 nm	*Proteus* spp., *Pseudomonas fluorescens*, and *Flavobacterium* spp.	Antibacterial activity	24	–	100	75 μg/μL = 75,000,-000 μg/ml	Umashankari et al. (2012)
Nanoshield-treated surface	–	–	–	Antibacterial activity	–	–	–	–	Michalikova et al. (2017)
Cadmium oxide	Chemically synthesized from cadmium sulfate using acetic acid	UV-vis spectrometry, TEM 30 nm	*S. aureus*	Antibacterial activity	24	–	100	20 μg/ml	Salehi et al. (2014)
Silver	Biotransformation of ionic silver to nanopariculate silver nanoparticles (AgNPs), utilizing the cell free extract of the bacterium, *P. plecoglossicida*	UV-vis spectrophotometry FTIR, XRD, and TEM Size: 15–160 nm at pH 7, 10–90 nm at pH 8, 10–55 nm at pH 9, and 2–30 nm for pH 11	MDR *A. baumannii*, *E. coli*, *P. aeruginosa*, and *Salmonella enterica*	Antibacterial activity	12	–	100	25–50 μg	Raman et al. (2017)
Aluminum oxide NPs (Al2O3 NPs)	Procured from Sigma-Aldrich St. Louis	SEM Size: 50 nm	*E. coli*	Antibacterial activity	24	Perforation of the bacterial cell membrane and leakage of the cytoplasmic contents as revealed by SEM, HRTEM, ATR-FTIR, and infrared	100	1000 μg/ml	Ansari et al. (2014)
Silver NPs functionalized by tetracycline	Biologically synthesized silver nanoparticles using actinomycete extract	TEM, EDX, and SAED	*Bacillus subtilis*	Antibacterial activity	24	–	100	AgNPs, 200 μg/ml Ag NPs TET, 50 μg/ml Ag^{2+}, 12.5 μg/ml	Rafińska et al. (2019)
Silver	Biologically synthesized by *Azadirachta indica*. AgNPs functionalized by *Cymbopogon citratus* Stapf., *Cymbopogon martini* Roxb., *Eucalyptus globulus* Labill.,	UV-vis spectrophotometry, TEM, FTIR, NP tracking and analysis (NTA) system, and Zetasizer	*S. aureus and E. coli*	Antibacterial activity In vivo wound healing in rabbits	48	–	100	100 μg/disc	Bansod et al. (2015)

Table 2 (continued)

Nanomaterial	Preparation of nanoparticles	NP characterization methods and properties	Target organisms	Form of application	NP exposure time (hr)	NPs mechanism of action	Efficacy (%)	Effective dose (μg/mL)	Ref
	A. indica Linn., and *Ocimum sanctum* Linn oil extracts	Size: 15–35 nm Zeta potential: − 31.2							
Titanium nanotubular surface topographies	Physical fabrication of titanium nanotubes by anodization (modification of titanium surfaces in nanotube topographies)	SEM, AFM, XRD Size: 20, 40, 60, or 80 nm	*Staphylococcus epidermidis* and *S. aureus*	Antibacterial activity	24	–	Reduced	–	Ercan et al. (2011)
Silver Nps	Silver nitrate encapsulated in a silver releasing biomaterial; the ultrashort peptides which can self-assemble in water to form hydrogels and then irradiated by UV to form encapsulated silver NPs	TEM Size: 10–20 nm	*E. coli*, *P. aeruginosa*, and *S. aureus*	Antibacterial activity and biocompatibility ex vivo study using human dermal fibroblasts	24	–	100 NPs 50 TET	10 mM = 1078.9 μg	Reithofer et al. (2014)
Zinc oxide nanoparticles	Obtained from Alfa Aesar, Ward Hill, MA and Mk Nano, Ontario, Canada	TEM and DLS Size: 20 and 60 nm but enhanced antibacterial activity in 20 nm NPs Zeta potential: − 21.9 mV	*S. aureus*	Antibacterial activity	24	Destruction of the cell membrane by liberation of ROS such as hydrogen peroxide as quantified by the Amplex red hydrogen			
peroxide/peroxidase assay kit	96–60 nm NPs and ultrasound 76–20 nm and US. Appr 53 NP alone	500 μg/ml	Seil and Webster (2012)						
Zinc oxide and titanium dioxide nanoparticles	ZnO-NPs synthesized by the sol-gel method	XRD, FETEM and DLS Size: Zn NP, 35 nm; Ti NPs, 13 nm	Oral *Streptococcus mitis*	Antibacterial activity and biofilm attenuation	72	Destruction of the cell membrane by liberation of ROS/oxidative stress as revealed by SOD assay	100, ZnNPs 74.8, reduction of biofilm activity, ZnNPs	200 μg/ml	Khan et al. (2016)
Silver zinc oxide NPs co-administered with rifampicin	AgZnO nanocrystals (AgZnONCs) chemically synthesized by decomposition of the precursor of oxalate method	XRD, FTIR, TEM, and SEM Size: 12 nm	*Mycobacterium tuberculosis*	Antibacterial activity and ex vivo cytotoxicity assay of AgZnONP against human macrophage cell lines (THP-1) using MTT cell proliferation assay	672	Synergism of AgNPs, ZnONPs, and rifampicin against			
rifampicin-insensitive			Jafari et al. (2017)						

Table 2 (continued)

Nanomaterial	Preparation of nanoparticles	NP characterization methods and properties	Target organisms	Form of application	NP exposure time (hr)	NPs mechanism of action	Efficacy (%)	Effective dose (μg/mL)	Ref
H37RvMtb phagocytized by THP-1 cell lines	AgZnO-rifampicin mixture killed 100 of bacteria in the macrophages, while AgZnO had 0% efficacy	512:1.25–8192:20 μg/ml							
Silver NPs	Silver NPs green synthesized by *Phyllanthus amarus* extract	UV-vis spectroscopy, TEM, EDX DLS, XRD, and FTIR. Size: 24 nm Morphology: spherical Zeta potential: − 11.9 mV	MDR *P. aeruginosa*	Antibacterial activity	24	–	100%	100 μg/ml	Singh et al. (2014)

Monocyte chemoattractant protein-1 (MCP-1) carrying interleukin-12 p70 (IL-12p70), nanocoatings on orthopedic implants (Li et al. 2010), and multilayer polypeptide nanoscale coatings loaded with IL-12 (Li et al. 2009) successfully provoked the body's natural immunity against open fracture *S. aureus* infections in rat models (Table 4).

Three research articles reported the use of nanoorganic compounds as bactericidal agents. Pluronic-based nanoself-assemblies of bacitracin A (Nano-BA_{P85}) (Hong et al. 2018) and zeolitic imidazolate framework (ZIF) nanodagger arrays (Yuan and Zhang 2017) rescued rats from *S. aureus* infections and killed 100% of microorganisms inoculated on the surface. Nanostructured polyurethane surface inhibited the growth of *Staphylococcus epidermidis*, *E. coli*, and *P. mirabilis* significantly (Yao et al. 2013) (Table 4).

Methods used in fabrication of nanoparticles

Out of the 22 studies using inorganic NPs, nine studies employed biological means to synthesize and functionalize NPs. Four studies used physical means, while three studies chemically synthesized NPs. However, four studies used NPs purchased from nanotech centers, while two studies did not outline the methods used in fabrication of the NPs (Table 2). All the 15 studies which used inorganic-organic nanopolymers except three employed chemical methods to synthesize the nanocomposites. Two studies used physical methods (UV irradiation to reduce metal ions within the composites into NPs), while in one study, purchased NPs were used to build the nanopolymer (Table 3).

Methods for characterizing nanoparticles

orty-four studies (89.8%) characterized NPs and nanocomposites using different platforms. Platforms used to determine the diameter and size distribution of the NPs included the transmission electron microscopy (TEM), scanning electron microscopy (SEM), field emission transmission electron microscopy (FETEM), and high-resolution transmission electron microscopy (HRTEM). Dynamic light scattering (DLS) was employed to determine the zeta potential and size distribution of NPs. Attenuated total reflectance Fourier transform-infrared (ATR-FTIR) spectroscopy, Fourier transform-infrared spectroscopy (FTIR), and atomic force microscopy

Table 3 (continued)

Nanoparticles	Preparation of nanoparticles	NP characterization and properties	Target organisms	Form of application	NP exposure time (hr)	Mechanism of action NPs	Efficacy (%)	Effective dose (μg/ml and mM)	Ref
					cytotoxicity assay of NAg-PLGA against pre-osteoblastic MC3T3-E1 cell line using MTT cell proliferation assay				
Zhenga et al. 2010									
Iron oxide NPs-oxytetracycline	Iron oxide NPs chemically synthesized by reducing $FeCl_3$ to nanoscale by $NaBH_4$. Iron oxide NPs-oxytetracycline complex was fabricated by suspension of 20 mg/ml of oxytetracycline hydrochloride in NPs solution	Size: 11 nm	–	Antibacterial activity-nanodrug/-oxytetracycline system in zebrafish (in vivo)	672	Delivery of antibiotics to target tissues infected by bacterial pathogens without causing significant stress response; no toxicity exhibited to the host cells	Efficiently delivered the antibiotic as revealed by HPLC better than the control		Chemello et al. (2016)
Ormostamp surfaces with nanopillar arrays	Nanometer-scale pillar structures on the Ormostamp polymer material fabricated by UV nanoreplication technology	SEM and AFM Size: 3.1–39.1 nm	*Staphylococcus aureus*	Antibacterial activity	2	–	100	$40\mu m^2$	Wu et al. (2018)
Gold Nps surface modified by polyelectrolyte (PAH) and silver	Silver (Ag) NPs were produced by photo irradiating of Ag-NO3 in Triton X-100	TEM Size: 20–30 nm	*Escherichia coli* and *Bacillus Calmette-Guérin*	Antibacterial activity	120	–	100	5–10 μg/ml	Zhou et al. (2012)
Cadmium tellurium (CdTe) titanium oxide (TiO_2)--CdTe-TiO_2 nanocomposite	CdTe-TiO2 nanocomposite capped with mercaptopropionic acid (MPA) and conjugated with semiconductor quantum dots (QDs) was synthesized by an organometallic route	XRD, FTIR, TEM, HRTEM, UV-vis diffuse reflectance spectoscopy (DRS) Size: TiO_2, 10–12 nm, and CdTe QDs, ~ 3–4 nm	*B. subtilis* and *E. coli*	Antibacterial activity	–	Cell membrane rapture and oozing of the cytoplasmic contents revealed by SEM. Biofilm formation disintegration and arrested by CdTe-TiO2 nancomposite (125 μg/-ml) through inhibition of quorum sensing	99.9 *E. coli* and *B. subttilis* plankton 60 *P. aeruginosa* biofilms	125 μg/ml CdTe-TiO2 nanocomposite, 250 μg/ml TiO2 Nps	Gholap et al. (2013)
Silver ion-doped calcium phosphate-based ceramic coating titanium prosthetic implants	Nanomaterial synthesized using wet chemical method	–	MRSA	Antibacterial activity In vivo experiment using rabbits	24	–	88.9 (8/9) and 1/9 for control	–	Kose et al. (2013)
Silver NPs-curcumin	Chemically synthesized using citric acid as a reducing agent	Size: 52 nm Zeta potential: − 20 MeV	*E. coli* and *P. aeruginosa*	Antibacterial activity synergism of Ag NPs and curcumin	24	–	100	0.024 mg/ml (24 μg/ml) AgNP 400 μg/ml of CUR	Alves et al. (2017)

Table 4 Organic nanomaterials used as bactericide agents or antibacterial agents delivery systems

Nanomaterial	Preparation of nanoparticles	Method of characterization	Target organisms	Form of application	NP exposure time (hr)	Mechanism of NP action	Efficacy (%)	Effective dose (μg/ml)	Ref
Pluronic-based nanoself-assemblies of bacitracin A (Nano--BA_{P85})	Thin-film hydration method	NICOMP™ 380 ZLS and TEM, DLS	*E. coli*, *S. typhimurium*, *P. aeruginosa*,- *S. aureus*, *Streptococcus pneumoniae, and Trueperella pyogenes*	Antibacterial activity	18	Membrane perforation as revealed by TEM imaging and imaging and fluorescent spectroscopy	100 in vitro 100 protection of rat model	0.5–2 μM (0.7114–2.85 μg/ml) for in vitro therapy 30 mg/kg (0.03 μg/mg) for in vivo therapy	Hong et al. (2018)
Nanoemulsions containing *Cymbopogon flexuosus*, lemongrass oil	Nanoencapsulation of *Cymbopogon flexuosus*. Lemongrass oil using homogenization method under high agitation to form nanoemulsions.	DLS, electrophoretic mobility technique, and TEM Size: 200 nm Zeta potential: -10.2 ± 0.34	*Cryptococcus grubii, P. aeruginosa*, and *S. aureus*	Nanodelivery system and antibacterial activity	24	–	100	0.28–1.33 mg/ml (280–1133 μg/ml), nanoemulsion 0.58–1.22 mg/ml (580–1220 μg/ml), oil alone	Da Silva Gündel et al. (2018)
Solid lipid nanoparticles containing *Eugenia caryophyllata* essential oil (SLN-EO)	High-shear homogenization and ultrasound methods. Encapsulation of *Eugenia caryophyllata* essential oil EO using glycerol monostearate (GMS), precirol, and stearic acid to for SLN-EO nanoemulsion	TEM, DLS, and DSC	*Salmonella typhi*, *Pseudomonas aeruginosa*, and *Staphylococcus aureus*	Antibacterial activity and antimicrobials delivery system	24	–	100	–	Fazly Bazzaz et al. (2018)
Monocyte chemoattractant protein-1 (MCP-1) and interleukin-12 p70 (IL-12p70) nanocoatings on orthopedic implants	Synthesis of MCP-1 and IL-12 p70 nanocoatings was prepared on stainless steel Kirschner wires (K wires) using electrostatic layer-by-layer self-assembly nanotechnology	SEM average thickness, 6 nm	MDR *Staphylococcus aureus*	Nanodelivery system to enhance antibacterial activity against open fracture *S. aureus* infections	504	Releases MCP-1 and IL-12 which enhances the body's natural defense systems to combat *S. aureus*	Decreased from 90 to 20	–	Li et al. (2010)
Multilayer polypeptide nanoscale coatings incorporating IL-12	Synthesis of IL-12 nanoscale coatings using electrostatic layer-by-layer self-assembly nanotechnology	UV-vis spectroscopy, ellipsometry, and SEM 7 nm	*Staphylococcus aureus*	Nanodelivery system to enhance antibacterial activity against open fracture *S. aureus* infections	504	Nanodelivery system releases IL-12 which enhances cell-mediated immunity in an open fracture rat model	80 decrease vs 10 for control	10.6 ng (0.0106 μg)	Li et al. (2009)
Chitosan NP loaded with ciprofloxacin- Cipro/-CSNPs	CSNPs were prepared by ionic cross-linking of chitosan with trisodium polyphosphate (TPP) (ionotropic gelation method)	FTIR spectra, XRD Size: 36.7 ± 3.59 nm to 114.36 ± 53.51 nm and 267.50 ± 4.99 nm after loading the drug Zeta potential: 0 to ± 5 mV, ± 10 to ± 30 mV, ± 30 to ± 40 mV, ± 40 to ± 60 mV	*E. coli*, *B. thuringiensis*, MRSA, and *P. aeruginosa*	Chitosan nanodelivery system of ciprofloxacin to promote its antibacterial activity	24	Chitosan nanodelivery system releases ciprofloxacin which enhances Cipro antibacterial activity	100	0.0043–0.14 μg/ml for *E. coli* and MRSA 0.03 μg/ml for CIPRO	Marei et al. (2018)
Carbon nanomaterial, graphene oxide	GO nanosheets were obtained from the Nanjing XFNANO Materials Tech Co., Ltd., China	XPS, AFM, UV spectroscopy, and FETEM Thickness of nano tubes:0.8–1 nm	Aquatic bacteria	GO nanodelivery system of sulfamethoxazole (SMZ) to promote its antibacterial activity	–	GO significantly inhibits the abundances of SMZ ARGs and the related *intI* gene by the formation of the p-DNA-GO	0		Zou et al. (2016)

Table 4 (continued)

Nanomaterial	Preparation of nanoparticles	Method of characterization	Target organisms	Form of application	NP exposure time (hr)	Mechanism of NP action	Efficacy (%)	Effective dose (μg/ml)	Ref
		Zeta potential: −31 to −43 mV				complex. The ARG abundances decreased with an increasing time of GO exposure			
Zeolitic imidazolate framework (ZIF) nanodagger arrays	Chemically synthesized by coating poly(methyl methacrylate) (PMMA) plate/glass/wood/-silicone rubber/copper foil/zinc			foil/polytetrafluoroethylene (PTFE) strip with ZIF. ZIF was chemically synthesized by reacting 2-methylimidazole (2-MeIm) to zinc ions molar ratio of 7	–	*E. coli* and *S. aureus*	Antibacterial activity (self--disinfecting/-antimicrobial surface)	24	–
PMMA-ZIF kill 100 of microorganisms inoculated on the surface	2.5 mg/ml = 2500 μg/ml	Yuan and Zhang (2017)							
Clavanin- methacrylate nanocarrier complex	Nanostructures were chemically prepared by mixing clavanin A and copolymer	AFM, SEM, and DLS Size: 120–372 nm Zeta potential: □7.16 mV	*S. aureus*, *K. pneumoniae*, and *P. aeruginosa*	Methacrylate nanocarrier delivery system of clavanin A to treat bacterial infections in mice	12	Methacrylate nanocarrier delivery system of clavanin promoted clavanin antibacterial activity	100 survival rate under sublethal sepsis assays 40 under lethal sepsis assays	0.2 μg	
/kg = 2×10^{-7} μg/mg	Saude et al. (2014)								
Oleic acid (OA)-monomethoxy polyethylene glycol (mPEG) nanocarrier for vancomycin (VM)/-mPEG-OA nanocarrier-VM complex	Oleic acid (OA) was coupled with monomethoxy polyethylene glycol (mPEG) to form mPER-OA nanocarrier and used to encapsulate vancomycin (VM) to form mPEG-OA-VM complex/VM-loaded mPEG-OA polymersomes	TEM and DLS Size: 142.9 nm Zeta potential: − 18.3 mV	MSSA and MRSA	mPEG-OA nanocarrier delivery system of vancomycin to treat bacterial infections in mice and skin infection models and ex vivo cytotoxicity of mPEG against human breast ade nocarcinoma (MCF 7), adenocarcinomic human alveolar basal epithelial cells (A 549), and human liver hepatocellular carcinoma 173 (HepG 2) using MTT cell proliferation assay	24	mPEG-OA nanocarrier delivery system of vancomycin promoted vancomycin antibacterial activity during in vivo therapy using mice model where 1.47-fold greater reduction in bacterial load after treatment with VM-loaded mPEG-OA polymersomes compared with bare VM registered in	VM, 92 and 90.5 for MSSA and MRSA, respectively VM-mPEG-OA, 90.5 and 86.8 for MSSA and MRSA, respectively	0.37 μg /ml of VM loaded mPEG-OA for MSSA 5.86 μg/ml of VM loaded mPEG-OA for MRSA 15.62 μg/ml of VM for MSSA 31.25 μg/ml for MRSA	Omolo et al. (2017)
Nanostructured polyurethane	Nanostructured polyurethane was chemically fabricated by soaking polyurethane polymers in nitric acid (HNO_3)	SEM and AFM Size: Bumps of 100 nm	*Staphylococcus epidermidis*, *E. coli*, and *P. mirabilis*	Antibacterial activity	1	Bacteria cell wall may be unable to conform to the topography of a material with nanoscale surface features, inhibiting the early stages of bacteria adhesion	Decreased bacterial population significantly	–	Yao et al. (2013)
Imipenem/cilastatin-loaded poly Ɛ-caprolactone (PCL) and polylactide--co-glycolide (PLGA) nanocapsules	Imipenem/cilastatin polymeric nanocapsules fabricated using double emulsion evaporation method	Bioscope catalyst-AFM and laser diffraction were used for particle analysis and zeta UV/visible	Imipenem-resistant *K. pneumoniae* and *P. aeruginosa*	Antibacterial activity and drug delivery system	24	–	78.4, *K. pneumoniae* 74, *P. aeruginosa*	IMP/PCL: 2.65 μg/ml for *K. pneumoniae* and 8.13 μg/ml for *P. aeruginosa.*	Shaaban et al. (2017)

Table 4 (continued)

Nanomaterial	Preparation of nanoparticles	Method of characterization	Target organisms	Form of application	NP exposure time (hr)	Mechanism of NP action	Efficacy (%)	Effective dose (μg/ml)	Ref
		spectroscopy, FTIR, and XRD Size: IMP/PCL NPs,132-± 20 nm and IMP/-PLGA, 348 ± 65 nm. Zeta potential: 17 ± 1.6 PCL and 15 ± 0.6 PLGA							

(AFM) were applied to analyze the conjugation or capping of nanoparticles with other substances. X-ray diffraction (XRD) and energy dispersive X-ray spectroscopy (EDX) were applied to determine the mineral content, size, and quality of NPs. Differential scanning calorimeter was used to determine the molecular stability of dilute in solution NPs. Thermogravimetric analysis (TGA) was performed to investigate the presence and amount of surface-bound ligand in nanohybrids. UV-visible diffuse reflectance spectroscopy (DRS) was applied to confirm the presence of metal elements; spectroscopic ellipsometry studied the optical properties of nanocomposites. X-ray photoelectron spectroscopy (XPS)/X-ray spectroscopy was used to measure the elemental composition within nanocomposites. UV visible spectroscopy was applied to predict the geometry of nanoparticles and to monitor the process of plant extract-mediated synthesis of NPs (Table 2, 3, and 4).

Characteristics of nanoparticles

Inorganic nanoparticles

Out of the 22 studies which used inorganic NPs, 17 reported the diameter size of NPs synthesized. The size of NPs ranged from 2 to 250 nm in diameter. Gold NPs displayed the smallest diameter (2–5 nm), while silver exhibited the biggest diameter (65–250 nm). Only four studies reported the zeta potential of NPs. Zeta potential varied from − 11.9 to − 31.2 mV. Eight articles reported the shapes of the metal NPs used. The shapes of NPs were spherical, irregular (Naz et al. 2013), triangular, and polygonal (Table 2).

Inorganic-organic nanohybrids

Sixty seven percent (67%) of the studies which investigated the potential of inorganic-organic nanohybrids as drug carriers or antibacterial agents reported the size of the nanocomponents of nanohybrids. The size ranged from 3 to 52 nm. The smallest nanocomponents were CdTe (3-4 nm) harbored in CdTe-TiO_2 nanocomposite, while silver-curcumin nanohybrid had the biggest NPs (Zhou et al. 2012). Zeta potential was documented in only three articles. Alves et al. (2017) reported negative zeta potential of − 20 mV in silver-curcumin composite,

while positive zeta potentials of + 8.9 mV in pSWCNT-Ag and + 39 mV in MNP-CSA-13 were registered. Only three studies characterized nanohybrids as spherical and conical (Table 3).

Nanoorganic molecules

All the studies which designed nanoorganic materials as nanovehicles for antibacterial agents determined their diameter, while 66.7% (8/12) reported their zeta potential. The diameter ranged from 0.8 to 1 nm in GO-carbon nanotubes to 397 ± 10.1 nm − 7 86.9 ± 11 nm in solid lipid nanodroplets loaded with *Eugenia caryophyllata* essential oil (SLN-EO). One study determined the diameter of the nanodelivery system before and after loading as 36.7 ± 3.59 nm, − 114.36 ± 55.31 nm, and 267.50 ± 4.99 nm, respectively, in the chitosan nanocarrier-ciprofloxacin complex. Hong et al. (2018) observed that BA_{P85} nanocomplex with a diameter of 73.3–99.4 nm degraded synthetic bacterial lipopolysaccharide (LPS) from liposome with a diameter of 7000 to 2000 nm. Shaaban et al. (2017) and Yuan and Zhang (2017) reported positive zeta potentials of 17 ± 1.6 mV for imipenem/cilastatin-loaded polycaprolactone (IMP-PCL) nanocapsule; 15 ± 0.6 mV for polylactide-co-glycolide filled with imipenem/cilastatin (IMP-PLGA), and 29 mV for zeolitic imidazolate framework (ZIF) nanodagger arrays, respectively. Six studies documented negative zeta potential with a lower limit of − 43 mV and upper limit of − 3.02 mV. For studies which determined the shape; nanoorganic materials were spherical (Table 4).

Nanomaterial exposure time

Among the studies included in this systematic review, 93.4% (46 out 49) documented the nanomaterial exposure time against bacteria isolates. The exposure time ranged from 0.67 (40 min) to 672 h (28 days) with an average of 48.8 h and model frequency of 24 h (Tables 2, 3, and 4).

Nanoparticle bactericidal mechanisms

Thirteen studies (26.5%) investigated the mechanism of action of NPs. The most common mechanisms included the disruption of the cell membrane leading to the leakage of the intracellular contents, downregulation of proteins, aggregation and melting of bacterial cells, failure of bacterial cells to adhere to the topography (bumps) of nanolayered surfaces, and inhibition of quorum sensing. These mechanisms were revealed through different platforms like, AFM, FESEM, SEM, TEM, EDX, HRTEM, and ART-FTIR in addition to peroxidase assay, superoxide dismutase (SOD) assay, and beta-galactosidase assay (Tables 2, 3, and 4).

Effective nanoparticle concentration/dose

The effective NP formulation concentration ranged from 2×10^{-7} μg/mg (clavanin-methacrylate nanocarrier complex) to 13,900 μg/ml for titanium oxide NPs (Tables 2, 3, and 4). For inorganic NPs, the lowest and highest effective doses were 0.5 μg/ml and 13,900 μg/ml, respectively. The effective concentration for organic NPs varied from 2×10^{-7} μg/mg to 2500 μg/mg, while for hybrid nanocomposites, the effective dose stretched from 7.5 to 10,789 μg/ml. The mean effective dose was highest for inorganic NPs (1361 μg/mg), followed by nanohybrids (905 μg/mg), and organic NPs had the lowest average effective dose of 357.8 μg/mg (Fig. 4). However, statistical analysis did not yield any significant difference in effective doses between inorganic NPs and organic NPs ($P = 0.66$), inorganic and nanohybrids ($P = 0.89$), and organic NPs against nanohybrids ($P = 0.9$). Interestingly, vancomycin alone and mPEG-OA nanocarrier loaded with vancomycin displayed similar efficacies against MSSA and MRSA isolates. However, the effective dose for the former was significantly lower (0.37 μg/mg and

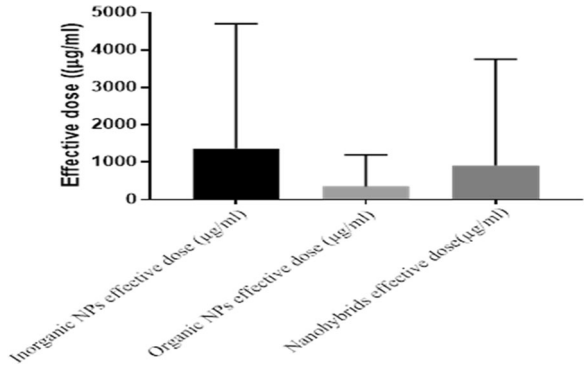

Fig. 4 Comparison of mean effective dose between inorganic, hybrid, and organic NPs. Tukey's multiple comparison test was used to compute and compare the mean effective dose. *P* values of 0.655 between inorganic NPs and organic NPs, 0.889 for inorganic versus nanohybrids, and 0.895 for organic NPs against nanohybrids were generated, revealing insignificant differences among the effective doses

5.86 μg/mg against MSSA and MRSA, respectively) than for the latter (15.62 μg/mg and 31.25 μg/mg against MSSA and MRSA, respectively).

Bactericidal efficacy of nanoparticles

Antibacterial efficacy of NPs ranged from 0% for GO nanodelivery system of sulfamethoxazole to 100% in 76.1% of the studies which reported efficacy (Tables 2, 3, and 4). The mode and median efficacy was 100%. Inorganic NPs registered the highest bactericide efficacy of 96.82%, followed by nanohybrid composites at 96.79% and trailed by nanoorganic molecules (83.3%). The overall mean bactericide efficacy of all categories of NPs was 94.7%. Nevertheless, multiple comparisons between inorganic and organic NPs ($P = 0.08$), inorganic versus nanohybrids ($P = 0.9$), and organic NP versus nanohybrid ($P = 0.1$) did not reveal any significant differences (Fig. 5). Furthermore, one study reported 100% and 17% efficacy of gold-copper NPs against *Bacillus anthracis* cells and *Bacillus anthracis* spores, respectively. Efficacies of silver NPs against antibiotic-sensitive and MDR *P. aeruginosa* biofilms were 67% and 56%, respectively. Five studies investigated the efficacy of NPs against bacterial biofilms (Tables 2 and 3). The NP antibacterial efficacy ranged from 50 to 100% with a mean value of 71.97%. Single-factor ANOVA revealed that NP efficacy against bacterial planktons and biofilms was significantly different ($P < 0.002$). It is worth noting that Jafari et al. (2017) observed a synergism between silver-zinc oxide NPs and rifampicin with efficacy of 100% against rifampicin-resistant H37RV Mtb

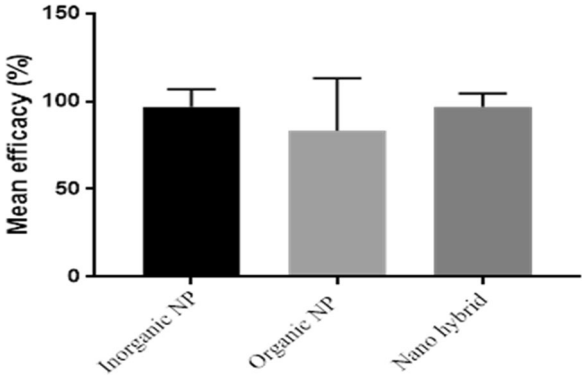

Fig. 5 Comparison of mean percentage efficacies between inorganic, hybrid, and organic NPs. Tukey's multiple comparison test was used to calculate and compare the mean percentage efficacies giving P values of 0.0833 for inorganic versus organic NPs, > 0.9999 for inorganic versus nanohybrids, and 0.1080 for organic NP versus nanohybrid, revealing considerable similarities

phagocytized by THR1 cell lines, while the latter and former individually exhibited 0% efficacy.

Nanoparticle toxicity

Nanoparticle biocompatibility studies were carried out in 14.3% of the studies. Ex vivo cytotoxicity assay of silver NPs, silver zinc oxide NPs, mPEG, PHEMA hydrogel, and Nag-PLGA were performed against human dermal fibroblasts (Reithofer et al. 2014), human macrophage cell line (THP-1) (Jafari et al. 2017), human breast adenocarcinoma (MCF7); adenocarcinoma human alveolar basal epithelial cells (A 539), human liver hepatocellular carcinoma (HepG 2) (Omolo et al. 2017), NIH-3 T3 fibroblasts (Xu et al. 2018), and preosteoblastic MC3T3-E1 cell line (Zhenga et al. 2010), respectively, using the MTT cell proliferation assay. Ex vivo cytotoxicity investigation of TPU-DA nanosilver complex was tested on HaCaT cells and NIH 3T3 fibroblasts using the CCK8 assay (Liu et al. 2018). In vivo toxicity of pSWCNT-Ag was done using chick embryos (Park et al. 2018). Results from all the biocompatibility assays exhibited that the nanomaterials were not toxic as cell viability of above 75% in the presence of nanotherapeutic agents was registered.

Discussion

Fabrication of organic nanoparticles

Synthesis of inorganic nanoparticles using traditional approaches such as chemical and physical methods has shortcomings. Physical approaches are not cost-friendly as they require exceedingly expensive equipment which use high energy, temperature, and pressure (Guzmán et al. 2009). Chemo-nanoparticle fabrication mainly entails wet chemistry where numerous reducing agents are employed to reduce metal salts to their nanoform in solutions (Tahir et al. 2013). The use of hazardous solvents and reducing agents during chemosynthesis results into contaminated NPs that are toxic to both target bacterial and host cells (Kawata et al. 2009). Moreover, several stabilizers are also required to prevent agglomeration of nanoparticles when in solution to functionalize and enhance their biocompatibility (Castro et al. 2014). To combat these drawbacks, novel, inexpensive, unsophisticated, and environmentally friendly biological approaches such as green synthesis of nanoparticles using plant extracts have been explored

(Huang et al. 2014). Plant extracts with antioxidant properties have gained immense attention owing to their ability to scavenge electrons from metal ions, thereby reducing them to their nanoscale as well as functionalizing them (Khan et al. 2013). This is in agreement with the majority of the studies which used inorganic nanoparticles included in this review. Among the 16 studies which synthesized in-house inorganic NPs, 56.3%, 25%, and 18.8% used biological, physical, and chemical methods, respectively. This clearly shows an inclination toward biosynthesis of inorganic NPs from their metal ions. Furthermore, biological approaches are becoming more popular in resources, facilities, and technical limited environments as they are cheap and eco-friendly and they yield functionalized non-toxic NPs.

Physicochemical properties of nanoparticles

The antibacterial activity of NPs depends on their physicochemical characteristics such as size, shape, and zeta potential. Minute NPs have very high chemical reactivity and bacterial cell wall and membrane penetrative power as compared with their bigger counterparts, hence potent bactericide effect on bacterial cells at very low minimum inhibitory concentration (MIC). Lu et al. (2013) reported silver NPs with a diameter of 5 nm exhibited the highest antimicrobial activity with a MIC value of 25 μg/ml. Furthermore, bactericidal action of the NPs is reliant on both size and shape; hence, variability in the mode of action of different forms of NPs may enlighten why resistance to this treatment is yet to be reported (Kvitek et al. 2008; Markova et al. 2012). Therefore, knowing the size and shape distribution of the NPs elucidates their efficacy. Zeta potential is an important aspect in the application of NPs as antimicrobial agents. Nanoparticles with a negative zeta potential tend to agglomerate to form bigger clusters when in solution, hence compromising their advantage over non-nanoforms, and they are repelled by a negative charge possessed by the bacterial cell membrane. On the other hand, NPs with a positive zeta potential singly remain in solution, and their positive charge is highly attracted to the negative charge of the bacterial cell membrane, thereby enhancing their adsorption to the bacterial cells. Therefore, zeta potential is a fundamental factor for the stability of nanoparticles in solution. A zeta potential of at least ± 30 is required for minimum NPs' stability (Muller et al. 2001). Fortunately, 89.9% of the studies included in this review characterized the NPs to determine their physicochemical characteristics using TEM, HRTEM, SEM FESEM, and DLS.

Drug nanodelivery systems

Peptides, lipids, antibodies, and cytokines have exhibited potent antimicrobial activity, but properties such as low solubility, short half-life, and bio-incompatibility in the circulatory system have hindered their pharmaceutical applicability (Pini et al. 2005). Nanoencapsulation as drug delivery systems augment therapeutic efficiency of these molecules by increasing their bioavailability and penetration across biological membranes. Furthermore, nanodelivery systems sustain controlled drug release, hence maintaining the required plasma drug concentration. Drug nanocarriers afford drugs a mechanism of evading the pathogens' molecular resistance mechanisms such as gained antibiotic resistance through alteration of the surface membrane proteins and protection against hydrolytic enzymes which degrade antibiotics (Devalapally et al. 2007; Sadurní et al. 2005). This is in agreement with the studies included in this systematic review which used nanobiotechnology to design drug delivery systems. Li et al. (2010, 2009) designed monocyte chemoattractant protein-1(MCP-1) and interleukin-12 p70 (IL-12p70) nanocoatings on orthopedic implants and multilayer polypeptide nanoscale coatings incorporating IL-12. These drug nanocarriers maintained the bioavailability and release of pro-inflammatory molecules. This technology provoked the cell-mediated immunity in open fractures of rat models, hence enhancing the immune-mediated cytotoxicity against MRD and sensitive *S. aureus* infections. Bismuth NPs conjugated with polyclonal *P. aeruginosa* antibodies enhanced their antibacterial activity against MDR *P. aeruginosa* with an efficacy of 90% as compared with 6% for the antibodies alone (Luo et al. 2013). Nanoencapsulation of clavanin A peptide with methacrylate (Saude et al. 2014), *C. flexuosus* oil with nanoemulsion (Da Silva Gündel et al. 2018), and *E. caryophyllata* essential oils with solid lipid NPs (Fazly Bazzaz et al. 2018) enhanced their antibacterial efficacy to 100% in in vivo and in vitro systems compared with the controls. Enhanced antibacterial activity of nanoencapsulated molecules may be attributed to their increased bioavailability as the nanocapsules protect them from the destabilizing factors of the external environment.

Chitosan loaded with ciprofloxacin (Marei et al. 2018), mPEG-OA nanocarrier encapsulating

vancomycin (Omolo et al. 2017), and nanoencapsulation of imipenem/cilastatin by polycaprolactone (PCL) and polylactide-co-glycolide (Shaaban et al. 2017) boosted the bactericidal effect of the antibiotics on sensitive and MDR bacteria. The high efficacy of antibiotics delivered by nanocapsules is attributed to the capability of nanocapsules to protect the drugs from the hydrolytic enzymes secreted by resistant bacteria. Moreover, encapsulated drugs such as carbapenems disguisedly diffuse across the cell membrane of resistant bacteria with mutant porins. Contrary to that, GO nanodelivery system of sulfamethoxazole (SMZ) considerably subdued the intracellular abundance of SMZ. GO augmented the diffusion of SMZ from the intracellular to the extracellular environment by increasing the cell membrane permeability. In addition, GO-SMZ complex reduced the uptake of SMZ into the bacteria (Zou et al. 2016).

Furthermore, to design a competent drug nanodelivery system, one needs to understand the mechanism of interaction between the nanovector and the drug, the conditions under which the drug will dissociate from the nanocarrier and hence its release and the combinatory effect of the nanocarrier and the drug. If there is no possible bondage, a linker between the nanocarrier and the drug or material to be delivered is a possible option. Among the articles included in this systematic review, two articles reported the application of a linker to form nanocarrier drug/material complex: Chatterjee et al. (2011) created an interaction between gold NPs and plasmid DNA using glutathione as a linker. Glutathione interacts electrostatically with both DNA and gold nanoparticle. The association with DNA is through free-end g-glutamine residue amine group which non-specifically interrelates with the negatively charged phosphate group of DNA, while the carboxyl group of glycine residue electrostatically interacts with the positively charged gold nanoparticle to form glutathione-functionalized gold nanoparticle. Therefore, the electrostatic interaction of gold NPs, glutathione, and DNA results into a reversible electrostatic gold-glutathione-DNA complex which releases DNA once inside the cell due to ionic variation. Hence gold-glutathione-plasmid DNA (with ampicillin-resistant gene) complex was designed and used to deliver ampicillin-resistant gene to *E. coli*. It is worth noting that gold NPs exhibited no growth inhibitory effect against *E. coli* at a very high concentration of 100 μg/ml there non-toxic but demonstrated potent material delivery activity hence a candidate for drug delivery.

In another study, Niemirowicz et al. (2015) fabricated a ceragenin-coated iron oxide magnetic NPs (MNP-CSA-13) hybrid. Despite the potent antimicrobial activity of ceragenin (CSA-13), a synthetic peptide, safety concerns due to its non-selective toxicity have limited its use (Lai et al. 2008). However, MNP-CSA-13 nanocomposite formed from the conjugation of iron oxide magnetic NPs (MNP) with CSA-13 targeted only *P. aeruginosa* biofilms and free-living cells at very high concentration of 100 μg/ml. No hemolysis of erythrocytes was observed showing that conjugation of synthetic peptides with nanocarriers minimizes host cytotoxicity (Zhao et al. 2009). The link between MNPs and CSA-13 was established through glutaraldehyde (Massart 1981). The treatment of MNPs with 3-aminopropyl trimethoxysilane (APTMS) results into a functional amino-terminated silica on the MNPs surface which reacts with glutaraldehyde. The terminal aldehyde groups on the MNP surface forms a platform for binding of CSA-13 where they react with the primary amine groups of CSA-13. MNP-CSA-13 might dissociate under low pH due to infection and inflammation. This potentiates the MNP-CSA-13 nanocomplex to dissociate and release CSA-13 antimicrobial peptide due to the hydrolysis of the imine bond at low pH. Therefore, MNP-CSA-13 is a promising nanodrug vector for pH-dependent conventional antimicrobial delivery/release to kill pathogens at infection sites where the pH is often lower than six (Kierys 2014).

Nanoparticle bactericidal mechanism of action

To date, the bactericidal mechanism of NPs is yet to be fully clarified. However, for inorganic NPs, it might reside within the capacity to discharge cations which irreversibly perforate bacterial cell wall, inactivate vital proteins, and chelate DNA or through generation of reactive oxygen species (ROS) (Slavin et al. 2017; Rizzello and Pompa 2014). Disintegration of the bacterial cell wall and membrane inhibition of protein synthesis were confirmed by some studies included in this review (Sowmya et al. 2018; Seil and Webster 2012; Ansari et al. 2014; He et al. 2016; Khan et al. 2016; Addae et al. 2014; Park et al. 2018; Su et al. 2011; Niemirowicz et al. 2015; Zanni et al. 2017; Gholap et al. 2013; Hong et al. 2018). In these studies, AFM, FESEM, SEM, TEM, EDX, HRTEM, and ART-FTIR

revealed that disintegration of the cell membrane was through puncturing action of NPs which is contrary to cations mediated degeneration of the cell membrane. Though two studies (Seil and Webster 2012; Khan et al. 2016) reported cell membrane collapse through liberation of ROS that seems to be arbitrated by the discharge of cations, this clearly explains why NPs and nanomaterials are the most promising candidates to supplement or be co-administered with antibiotics. When NPs inactivate vital proteins, chelate DNA, and inhibit protein synthesis, bacterial cells become incapacitated to launch any molecular mechanism of antibiotic resistance as such mechanisms totally depend on the metabolic pathways and cellular structures affected by the nanomaterials.

Shift from ultraviolet to visible light responsiveness

Traditionally, the antibacterial activity of titanium lies in its activation by ultraviolet (UV) light illumination. This limits the application of titanium-based compounds as antibacterial agents in vivo since the catalyst UV light is invasive to mammalian cells. Therefore, its applicability as a bactericidal agent is restricted to abiotic environments. However, titanium in nanoscale form can be modified to shift from low wavelength absorption spectrum to higher wavelength as revealed by three studies included in this review. Gholap et al. (2013) conjugated TiO_2 NPs to CdTe QDs, Senarathna et al. (2017) capped TiO_2 NPs with *Garcinia zeylanica* extract, and Cheng et al. (2009) coated nanostructured TiO_2 powder with carbon. These surface modifications of TiO_2 NPs transferred the bactericide activity of TiO_2 photocatalyst from UV light to visible light responsive. Therefore, the induced ability of TiO_2 in its nanoform through surface manipulation to absorb light from the visible spectrum highlights its possible applicability as an antimicrobial agent in biotic environments.

Nanoparticle bactericidal efficacy versus dose

The bactericidal efficacy of a number of antimicrobial agents is dose dependent (McKenzie 2011; Levison and Levison 2009). However, high concentrations exhibit non-selective cytotoxicity. Therefore, therapeutic agents with very low minimum inhibitory concentration (MIC) and minimum bactericidal concentration (MBC) are preferred. Nanoscale molecules present very high chemical reactivity, solubility, and hence more efficacious bacteria inhibitory effect at very low concentrations as compared with their non-nanoscale forms (Slavin et al. 2017). These attributes made them the preferred future antimicrobials and antimicrobial carriers. Intensive research is being carried out to develop and assess nanomolecules as possible antibacterial alternatives and potentiators of bactericidal agents as carriers. Contrary to this, most studies incorporated in this review observed that nanomolecule bacterial growth inhibitory efficacy is dose dependent with mean effective concentrations of 357.8 μg/mg, 905 μg/mg, and 1361 μg/mg for organic NPs, nanohybrids, and inorganic NPs, respectively. These means are way above the recommended NP non-toxic dose (100 μg/mg) to mammalian cells. Surprisingly, Jafari et al. (2017) and Reithofer et al. (2014) reported that Ag NPs and AGZnO nanocrystals were non-toxic to mammalian cell lines at very high concentrations of 1078.9 and 512–8192 μg/mg in ex vivo experiments. Articles included in this review presented undisputable potent NP antibacterial efficacy against antibiotic-resistant and sensitive clinical isolates as revealed by the mean (94.7%), median (100%), and mode (100%) efficacies of in vitro and in vivo therapy. For safety concerns, the stumbling block lies in the formulation of nanotherapeutic agents with efficacious biocompatible doses in in vivo systems.

Efficacy of nanoparticles against bacterial biofilms and spores

Bacterial biofilms are known to be exceedingly tolerant and resistant to antibiotics as they provide optimal environments for transfer of plasmids harboring antibiotic resistance genes via conjugation as well as the biofilm matrix protecting bacteria cells in lower films against antibiotics (Lowy 2003; Warnes et al. 2012; Ceri et al. 1999). Inorganic and organic nano-ordered surfaces and coatings are presently topping the options for medical device surface modification to prevent biofilm formation (Rizzello and Pompa 2014; Taylor and Webster 2011; Nair and Laurencin 2008). This conclusion is in agreement with the investigations of Yao et al. (2013) and Yuan and Zhang (2017) where zeolitic imidazolate framework (ZIF), nanodagger arrays, and nanostructured polyurethane significantly prevented the formation of *Staphylococcus epidermidis*, *E. coli*, *P. mirabilis*, and *S. aureus* biofilms perhaps by the failure of bacterial cell to conform to the topography of the nanolayered surface. Conversely, NP

formulations aimed at eradicating already formed biofilms yielded unpromising results comparable with antibiotics with bactericide efficacies as low as 50% and mean efficacy of 71.97%. Additionally, gold-copper sulfide NPs were ineffective against *Bacillus anthracis* spores at very high concentration (1081 μg/ml) (Addae et al. 2014). This is analogous with conclusions from other studies which used antibiotics (Louie et al. 2012).

Nanomaterial exposure time against bacteria

One of the factors influencing the evolution of antimicrobial resistance is the exposure time of antimicrobial agents against pathogens. Graves et al. (2015) observed that the consequential resistance to Ag NPs in *E. coli* was acquired by the 200th generation equivalent to over 10 days of exposure. However, the mode and average exposure times in articles included in this systematic review were 24 h and 48.8 h corresponding to approximately 6.5 and 13 generations, respectively. This might be the reason why high nanomaterial bactericidal efficacies were attained against clinical isolates in in vitro and in vivo experiments.

Biocompatibility studies

For safety reasons, it is a prerequisite to assess the toxicity level of any novel potential therapeutic agents using mammalian cells (Choksakulnimitr et al. 1995). This can be achieved by exposing the cells to the new therapeutic agent and cell viability computed using cytotoxicity calorimetric assays such as 3-(4,5-dimethylthiazol-2-yl)-2,5-diphenyltetrazolium bromide (MTT), 2,3-bis-(2-methoxy-4-nitro-5-sulfophenyl)-2H-tetrazolium-5-carboxanilide (XTT), and Cell Counting Kit-8 (CCK8). MTT, XXT, and CCK8 are tetrazolium yellow dyes. The principle behind these calorimetric assays lies in the ability of viable cells to reduce the yellow tetrazolium salt to formazan, an insoluble deep purple crystalline product. The intensity of the deep purple color formed in cells is directly proportional to the number of viable cells and can be assayed calorimetrically. This is because the activity of NADH-/NADPH-dependent oxidoreductase enzymes that reduce the MTT, XTT, and CCK8 dyes is maintained. To complement ex vivo experiments, in vivo cytotoxicity assays can be carried out by injecting nanoparticle formulations into embryos of model organisms followed by assessing their survival. This is in agreement with only 14.3% of the studies included in this systematic review. These studies reported cell viability of above 75% in the presence of nanotherapeutic agents comparable with the controls. Cell viabilities of 75% are considered to be biocompatible to mammalian cells (Hamid et al. 2004; Mosmann 1983). The similar reduction of cell viability of up to 25% in mammalian cell lines treated with nanoparticles and controls can therefore be attributed to alteration in local cellular microenvironment. However, Jafari et al. (2017) and Liu et al. (2018) observed that cell viability decreased with increasing concentration of nanoparticles administered. This is an indicator that high nanoparticle concentration compromises biocompatibility. Therefore, as a biosafety measure, NP formulations require very minute concentration but with potent antibacterial activity.

Conclusion

Due to the ever-increasing prevalence of antimicrobial resistance to old and newly synthesized drugs, alternative antimicrobials to replace or supplement available drugs are needed. The importance of nanotechnology in developing alternative antibacterial agents and antimicrobial enhancers such as nanocarriers has been confirmed in both in vitro and in vivo models. Studies assessed in this review revealed high bactericidal efficacies of organic, inorganic, and hybrid NPs. Notable example is where imipenem nanocarrier augmented its antibacterial effect against carbapenem-resistant clinical isolates. However, bactericidal efficacy of NPs is dose dependent necessitating the use of high concentration of NPs way above the MIC to achieve potent treatment outcomes albeit with non-selective toxicity. Therefore, there is still a limitation of formulating effective concentration of antibacterial nanotherapeutic agents that are biocompatible in in vivo systems. Furthermore, ROS generated by bacterial cells may not only disintegrate the bacterial cell membrane but also rapture the host cell membrane. As a safety precaution, in vitro, ex vivo, and in vivo cytotoxicity assays should be conducted to guarantee the safety of patients.

Acknowledgments We are thankful to MAPRONANO ACE for funding this work.

Availability of data and materials All relevant data has been submitted with the manuscript and therefore no supplementary data.

Authors' contributions This work was carried out in collaboration between all authors. Eddie Wampande (EW), Lubwama Michael (LM), Kirabira John Baptist (KJB), Dennis K Byarugaba (DKB), Robert Tweyongyere (RB), and Francis Ejobi (FB) conceptualized and designed the format for this systematic review. Kenneth Ssekatawa (KS), Charles Kato Drago (CKD), and EW performed the literature search and data analysis. All authors drafted the section of literature review. KS, EW, LM, KJB, and CKD wrote the first draft of the manuscript and managed manuscript revisions. All authors read and approved the final manuscript.

Funding information The authors declare that this systematic review was funded by Africa Centre of Excellence in Materials, Product Development and Nanotechnology, MAPRONANOACE Makerere University. This study was also funded in part by the Swedish International Development Cooperation Agency (Sida) and Makerere University under Sida Contribution No: 51180060. The grant is part of the European and Developing Countries Clinical Trials Partnership (EDCTP2) program supported by the European Union.

Compliance with ethical standards

Competing interests The authors declare that they have no competing interests.

Ethics and consent to participate Not applicable.

Consent for publication Not applicable.

Abbreviations *MDR,* Multidrug resistant; *MRSA,* Methicillin-resistant *Staphylococcus aureus*; *MSSA,* Methicillin-sensitive *Staphylococcus aureus*; *CRE,* Carbapenem-resistant *Enterobacteriaceae*; *AMR,* Antimicrobial resistance; *IS,* Insertion sequence; *NP,* Nanoparticles; *MIC,* Minimum inhibitory concentration; *MBC,* Minimum bactericidal concentration; *PDR,* Pan drug resistant; *ANOVA,* Analysis of variance; *μg,* Microgram; *ml,* Milliliter; *TPU,* Thermoplastic polyurethane; *DA,* Polydopamine; *NS,* Nanosilver; *pSWCNT-Ag,* Pegylated silver-coated single-walled carbon nanotubes; *SWCNT-Ag,* Silver-coated single-walled carbon nanotubes; *PHEMA,* Polyhydroxyethyl methacrylate; *BMP-2,* Bone morphogenetic protein 2; *PLGA,* Poly-DL-lactic-co-glycolic acid; *PAH,* Polyelectrolyte; *MNP-CSA-13,* Ceragenin-coated iron oxide magnetic NPs; *CSA-13,* Ceragenin 13; *ZNG,* Zinc oxide nanorods-graphene nanoplatelets; *DMAP-PTA,* Dimethyl amino pyridine propylthioacetate; *CdTe,* Cadmium tellurium; *TiO_2,* Titanium oxide; *MPA,* Mercaptopropionic acid; *QD,* Quantum dots; *SLN,* Solid lipid nanoparticles; *EO,* Essential oil; *Cipro,* Ciprofloxacin; *CSNP,* Chitosan nanoparticles; *mPEG,* Monomethoxy polyethylene glycol; *OA,* Oleic acid; *PCL,* Poly Ɛ-caprolactone; *GO,* Graphene oxide; *SMZ,* Sulfamethoxazole; *MCP-1,* Monocyte chemoattractant protein-1; *IL,* Interleukin; *BA,* Bacitracin A; *ZIF,* Zeolitic imidazolate framework; *TEM,* Transmission electron microscopy; *SEM,* Scanning electron microscopy; *FETEM,* Field emission transmission electron microscopy; *HRTEM,* High-resolution transmission electron microscopy; *DLS,* Dynamic light scattering; *ATR-FTIR,* Attenuated total reflectance Fourier transform-infrared spectroscopy; *FTIR,* Fourier transform-infrared spectroscopy; *AFM,* Atomic force microscopy; *XRD,* X-ray diffraction; *EDX,* Energy dispersive X-ray spectroscopy; *DSC,* Differential scanning calorimeter; *TGA,* Thermogravimetric analysis; *DRS,* UV-visible diffuse reflectance spectroscopy; *XPS,* X-ray photoelectron spectroscopy; *SOD,* Superoxide dismutase; *Mtb, Mycobacterium tuberculosis; ROS,* Reactive oxygen species; *MTT,* (Dimethylthiazol-2-yl)-2,5-diphenyltetrazolium bromide; *XTT,* 2,3-bis-(2-methoxy-4-nitro-5-sulfophenyl)-2H-tetrazolium-5-carboxanilide (XTT); *CCK,* Cell Counting Kit-8; *UV,* Ultraviolet

References

Addae et al (2014) Investigation of antimicrobial activity of photothermal therapeutic gold/copper sulfide core/shell nanoparticles to bacterial spores and cells. J Biol Eng 8:11. https://doi.org/10.1186/1754-1611-8-11

Ali SW, Joshi M, Rajendran S (2011) Synthesis and characterization of chitosan nanoparticles with enhanced antimicrobial activity. Int J Nanosci 10(4 & 5):979–984. https://doi.org/10.1142/S0219581X1100868X

Alves TF, Chaud MV, Grotto D, Jozala AF, Pandit R, Rai M, dos Santos CA (2017) Association of silver Nanoparticles and curcumin solid dispersion: antimicrobial and antioxidant properties. AAPS PharmSciTech 19(1):225–231. https://doi.org/10.1208/s12249-017-0832-z

Ansari MA, Khan HM, Khan AA, Cameotra SS, Saquib Q, Musarrat J (2014) Interaction of Al2O3 nanoparticles withEscherichia coli and their cell envelope biomolecules. J Appl Microbiol 116(4):772–783. https://doi.org/10.1111/jam.12423

Anwar A, Khalid S, Perveen S, Ahmed S, Siddiqui R, Khan NA, Shah MR (2018) Synthesis of 4-(dimethylamino) pyridine propylthioacetate coated gold nanoparticles and their antibacterial and photophysical activity. Nanobiotechnol 16:6. https://doi.org/10.1186/s12951-017-0332-z

Asadishad B, Hidalgo G, Tufenkji N (2012) Pomegranate materials inhibit flagellin gene expression and flagellar-propelled motility of uropathogenic Escherichia coli strain CFT073. FEMS Microbiol Lett 334:87–94

Asgarali A, Stubbs KA, Oliver A, Vocadlo DJ, Mark BL (2009) Inactivation of the glycoside hydrolase NagZ attenuates antipseudomonal-lactam resistance in Pseudomonas aeruginosa. Antimicrob Agents Chemother 53:2274–2282

Bansod SD, Bawaskar MS, Gade AK, Rai MK (2015) Development of shampoo, soap and ointment formulated by green synthesised silver nanoparticles functionalised with antimicrobial plants oils in veterinary dermatology: treatment and prevention strategies. IET Nanobiotechnol 9(4):165–171. https://doi.org/10.1049/iet-nbt.2014.0042

Billal DS, Feng J, Leprohon P, Legare D, Ouellette M (2011) Whole genome analysis of linezolid resistance in Streptococcus pneumoniae reveals resistance and compensatory mutations. BMC Genomics 12:512

Brody T, Yavatkar AS, Lin Y, Ross J, Kuzin A et al (2008) Horizontal gene transfers link a human MRSA pathogen to contagious bovine mastitis bacteria. PLoS One 3(8):e3074. https://doi.org/10.1371/journal.pone.0003074

Burygin G, Khlebtsov B, Shantrokha A, Dykman L, Bogatyrev V, Khlebtsov N et al (2009) On the enhanced antibacterial activity of antibiotics mixed with gold nanoparticles. Nanoscale Res Lett 4:794–801. https://doi.org/10.1007/s11671-009-9316-8

Castro L, Blázquez ML, González FG, Ballester A (2014) Mechanism and applications of metal nanoparticles prepared by bio-mediated process. Rev Adv Sci Eng 3:199–216

CDC (2013) Antibiotic resistance threats in the United States

Centre for Disease Dynamics, Economics and Policy (CDDEP) (2015) The state of the world's antibiotics. Washington DC-New Delhi

Ceri H, Olson ME, Stremick C (1999) The Calgary biofilm device: new technology for rapid determination of antibiotic susceptibilities of bacterial biofilms. J Clin Microbiol 37:1771–1776

Chan BK, Sistrom M, Wertz JE, Kortright KE, Narayan D, Turner PE (2016) Phage selection restores antibiotic sensitivity in MDR Pseudomonas aeruginosa. Nat Sci Rep 6:26717. https://doi.org/10.1038/srep26717

Chatterjee et al (2011) Effect of iron oxide and gold nanoparticles on bacterial growth leading towards biological application. J Nanobiotechnol 9:34. https://doi.org/10.1186/1477-3155-9-34

Chemello G, Piccinetti C, Randazzo B, Carnevali O, Maradonna F, Magro M, Olivotto I (2016) Oxytetracycline delivery in adult female zebrafish by iron oxide nanoparticles. Zebrafish 13(6):495–503. https://doi.org/10.1089/zeb.2016.1302

Cheng et al (2009) The effects of the bacterial interaction with visible-light responsive titania photocatalyst on the bactericidal performance. J Biomed Sci 16:7. https://doi.org/10.1186/1423-0127-16-7

Choi SJ, Oh JM, Choy JH (2010) Biocompatible nanoparticles intercalated with anticancer drug for target delivery: pharmacokinetic and biodistribution study. J Nanosci Nanotechnol 10:2913–2916

Choksakulnimitr S, Masuda S, Tokuda H, Takakura Y, Hashida M (1995) In vitro cytotoxicity of macromolecules in different cell culture systems. J Control Release 34:233–241

Colonna C, Conti B, Perugini P, Pavanetto F, Modena T (2007) Chitosan glutamate nanoparticles for protein delivery: development and effect on prolidase stability. J Microencapsul 24:553–564

Cui L, Chen P, Chen S, Yuan Z, Yu C, Ren B, Zhang K (2013) In situ study of the antibacterial activity and mechanism of action of silver nanoparticles by surface-enhanced Raman spectroscopy. Anal Chem 85:5436–5443

Da Silva Gündel S, de Souza ME, Quatrin PM, Klein B, Wagner R, Gündel A, Ourique AF (2018) Nanoemulsions containing Cymbopogon flexuosus essential oil: development, characterization, stability study and evaluation of antimicrobial and antibiofilm activities. Microb Pathog 118:268–276. https://doi.org/10.1016/j.micpath.2018.03.043

de la Fuente JM, Grazu V (2012) Nanobiotechnology, inorganic nanoparticles vs organic nanoparticles. Frontiers of nanoscience, vol 4. Elsevier Ltd

Devalapally H, Chakilam A, Amiji MM (2007) Role of nanotechnology in pharmaceutical product development. J Pharm Sci 96:2547–2565. https://doi.org/10.1002/jps

Economou V, Gousia P (2015) Agriculture and food animals as a source of antimicrobial-resistant bacteria. NCBI, Dove Medicine Press. Infect Drug Resist 8:49–61

Ercan B, Taylor E, Alpaslan E, Webster TJ (2011) Diameter of titanium nanotubes influences anti-bacterial efficacy. Nanotechnology 22(29):295102. https://doi.org/10.1088/0957-4484/22/29/295102

Fazly Bazzaz BS, Khameneh B, Namazi N, Iranshahi M, Davoodi D, Golmohammadzadeh S (2018) Solid lipid nanoparticles carrying Eugenia caryophyllata essential oil: the novel nanoparticulate systems with broad-spectrum antimicrobial activity. Lett Appl Microbiol 66(6):506–513. https://doi.org/10.1111/lam.12886

Gao W et al (2010) Two novel point mutations in clinical Staphylococcus aureus reduce linezolid susceptibility and switch on the stringent response to promote persistent infection. PLoS Pathog 6:e1000944

Gao W, Chen Y, Chang Y, Zhang Y, Chang Q, Zhang L (2018) Nanoparticle-based local antimicrobial drug delivery. Adv Drug Deliv Rev 127:46–57. https://doi.org/10.1016/j.addr.2017.09.015

Gholap H, Patil R, Yadav P, Banpurkar A, Ogale S, Gade W (2013) CdTe–TiO2nanocomposite: an impeder of bacterial growth and biofilm. Nanotechnology 24(19):195101. https://doi.org/10.1088/0957-4484/24/19/195101

Graves JL, Tajkarimi M, Cunningham Q, Campbell A, Nonga H, Harrison SH, Barrick JE (2015) Rapid evolution of silver nanoparticle resistance in Escherichia coli. Front Genet 6:42. https://doi.org/10.3389/fgene.2015.00042

Gulmez D, Woodford N, Palepou MF, Mushtaq S, Metan G, Yakupogullari Y, Kocagoz S, Uzun O, Hascelik G.& Livermore DM. (2008) Carbapenem-resistant Escherichia coli and Klebsiella pneumoniae isolates from Turkey with OXA-48-like carbapenemases and outer membrane protein loss. Int J Antimicrob Agents 31:523–526

Guzmán MG, Dille J, Godet S (2009) Synthesis of silver nanoparticles by chemical reduction method and their antibacterial activity. Int J Chem Biomol Eng 2:104–111

Hamid R, Rotshteyn Y, Rabadi L, Parikh R, Bullock P (2004) Comparison of alamar blue and MTT assays for high through-put screening. Toxicol in Vitro 18:703–710

Hausner M, Wuertz S (1999) High rates of conjugation in bacterial biofilms as determined by quantitative *in situ* analysis. Appl Environ Microbiol 65(8):3710–3713

He et al (2016) Study on the mechanism of antibacterial action of magnesium oxide nanoparticles against foodborne pathogens. Nanobiotechnol 14:54. https://doi.org/10.1186/s12951-016-0202-0

Hinchliffe P, Symmons MF, Hughes C, Koronakis V (2013) Structure and operation of bacterial tripartite pumps. Annu Rev Microbiol 67:221–242

Hofmann D, Messerschmidt C, Bannwarth MB, Landfester K, Mailander V (2014) Drug delivery without nanoparticle uptake: delivery by a kiss-andrun mechanism on the cell membrane. Chem Commun (Camb) 50:1369–1371

Høiby N, Bjarnsholt T, Givskov M (2010) Antibiotic resistance of bacterial biofilms. Int J Antimicrob Agents 35:322–332

Hong W, Liu L, Zhao Y, Liu Y, Zhang D, Liu M (2018) Pluronic-based nano-self-assemblies of bacitracin a with a new mechanism of action for an efcient in vivo therapeutic effect against bacterial peritonitis. J Nanobiotechnol 16:66. https://doi.org/10.1186/s12951-018-0397-3

Hou Y, Hu J, Park H, Lee M (2012) Chitosan-based nanoparticles as a sustained protein release carrier for tissue engineering applications. J Biomed Mater Res A 100:939–947

Huang L, Weng X, Chen Z, Megharaj M, Naidu R (2014) Green synthesis of iron nanoparticles by various tea extracts: comparative study of the reactivity. Spectrochim Acta A Mol Biomol Spectrosc 130:295–301

Islam et al (2017) A multi-target therapeutic potential of *Prunus domestica* gum stabilized nanoparticles exhibited prospective anticancer, antibacterial, urease-inhibition, anti-inflammatory and analgesic properties. BMC Complement Altern Med 17: 276. https://doi.org/10.1186/s12906-017-1791-3

Ivask A, El Badawy A, Kaweeteerawat C, Boren D, Fischer H, Ji Z et al (2014) Toxicity mechanisms in *Escherichia coli* vary for silver nanoparticles and differ from ionic silver. ACS Nano 8:374–386

Iyamba J-ML, Wambale JM, Lukukula CM, Takaisi-Kikuni NB (2014) High prevalence of methicillin resistant staphylococci strains isolated from surgical site infections in Kinshasa. Pan Afr Med J 18:322. https://doi.org/10.11604/pamj.2014.18.322.4440

Jafari A, Jafari Nodooshan S, Safarkar R, Movahedzadeh F, Mosavari N, Novin Kashani A, Majidpour A (2017) Toxicity effects of AgZnO nanoparticles and rifampicin on mycobacterium tuberculosis into the macrophage. J Basic Microbiol 58(1):41–51. https://doi.org/10.1002/jobm.201700289

Jahnke JP, Cornejo JA, Sumner JJ, Schuler AJ, Atanassov P, Ista LK (2016) Conjugated gold nanoparticles as a tool for probing the bacterial cell envelope: the case of *Shewanella oneidensis* MR-1. Biointerphases. 11:11003

Kawata K, Osawa M, OkabeS (2009) In vitro toxicity of silver nanoparticles at noncytotoxic doses to HepG2 human hepatoma cells. Environ Sci Technol 43:6046–6051

Khan M, Khan M, Adil SF, Tahir MN, Tremel W, Alkhathlan HZ, Al-Warthan A, Siddiqui MRH (2013) Green synthesis of silver nanoparticles mediated by Pulicaria glutinosa extract. Int J Nanomedicine 8:1507–1516

Khan ST, Ahmad J, Ahamed M, Musarrat J, Al-Khedhairy AA (2016) Zinc oxide and titanium dioxide nanoparticles induce oxidative stress, inhibit growth, and attenuate biofilm formation activity of Streptococcus mitis. J Biol Inorg Chem 21(3): 295–303. https://doi.org/10.1007/s00775-016-1339-x

Khan I, Saeed K, Khan I (2017) Nanoparticles: Properties, applications and toxicities. Arab J Chem 12:908–931. https://doi.org/10.1016/j.arabjc.2017.05.011

Kierys A (2014) Synthesis of aspirin-loaded polymer-silica composites and their release characteristics. ACS Appl Mater Interfaces 6(16):14369–14376

Kose N, Otuzbir A, Peksen C, Kiremitc A, Dogan A (2013) A silver ion-doped calcium phosphate-based ceramic nanopowder-coated prosthesis increased infection resistance. Clin Orthop Relat Res 471:2532–2539. https://doi.org/10.1007/s11999-013-2894-x

Kvitek A, Panacek J, Soukupova M, Kolar R, Vecerova R, Prucek M, Holecova R (2008) ZborilEffect of surfactants and polymers on stability and antibacterial activity of silver nanoparticles (NPs) J. Phys Chem C 112:5825–5834

Lai XZ, Feng Y, Pollard J, Chin JN, Rybak MJ, Bucki R, Epand RF, Epand RM, Savage PB (2008) Ceragenins: cholic acidbased mimics of antimicrobial peptides. Acc Chem Res 41(10):1233–1240

Lai H-Z, Chen W-Y, Wu C-Y, Chen Y-C (2015) Potent antibacterial nanoparticles for pathogenic bacteria. ACS Appl Mater Interfaces 7:2046–2054

Lavigne JP, Sotto A, Nicolas-Chanoine MH, Bouziges N, Pagès JM, Davin-Regli A (2013) An adaptive response of Enterobacter aerogenes to imipenem: regulation of porin balance in clinical isolates. Int J Antimicrob Agents 41: 130–136

Levison ME, Levison JH (2009 December) Pharmacokinetics and pharmacodynamics of antibacterial agents. Infect Dis Clin N Am 23(4):791–vii. https://doi.org/10.1016/j.idc.2009.06.008

Li B, Jiang B, Boyce BM, Lindsey BA (2009) Multilayer polypeptide nanoscale coatings incorporating IL-12 for the prevention of biomedical device-associated infections. Biomaterials 30(13):2552–2558. https://doi.org/10.1016/j.biomaterials.2009.01.042

Li B, Jiang B, Dietz MJ, Smith ES, Clovis NB, Rao KMK (2010) Evaluation of local MCP-1 and IL-12 nanocoatings for infectionprevention in open fractures. J Orthop Res 28(1). https://doi.org/10.1002/jor.20939

Li M, Zhu L, Lin D (2011) Toxicity of ZnO nanoparticles to *Escherichia coli*: mechanism and the influence of medium components. Environ Sci Technol 45:1977–1983

Li H, Luo YF, Williams BJ, Blackwell TS, Xie CM (2012) Structure and function of OprD protein in *PseudoImonas aeruginosa*: from antibiotic resistance to novel therapies. Int J Med Microbiol 302:63–68

Liu et al (2018) Nano-silver-incorporated biomimetic polydopamine coating on a thermoplastic polyurethane porous nanocomposite as an efficient antibacterial wound dressing. J Nanobiotechnol 16:89. https://doi.org/10.1186/s12951-018-0416-4

Livermore DM, Warner M, Mushtaq S, Doumith M, Zhang J, Woodford N (2011) What remains against carbapenem resistant *Enterobacteriaceae*? Evaluation of chloramphenicol, ciprofoxacin, colistin, fosfomycin, minocycline, nitrofurantoin, temocillin and tigecycline. Int J Antimicrob Agents 37:415–424

Long KS, Poehlsgaard J, Kehrenberg C, Schwarz S, Vester B (2006) The Cfr rRNA methyltransferase confers resistance to phenicols, lincosamides, oxazolidinones, pleuromutilins, and streptogramin A antibiotics. Antimicrob Agents Chemother 50:2500–2505

Loomba PS, Taneja J, Mishra B (2010) Methicillin and vancomycin resistant *S. aureus* in hospitalized patients. J Global Infect

Dis 2(3):275–283. https://doi.org/10.4103/0974-777X.68535

Louie A, VanScoy BD et al (2012) Impact of spores on the comparative efficacies of five antibiotics for treatment of Bacillus anthracis in an in vitro hollow fiber pharmacodynamics model. Antimicrob Agents Chemother 56:1229–1239

Lowy FD (2003) Antimicrobial resistance: the example of Staphylococcus aureus. J Clin Invest 111:1265–1273. https://doi.org/10.1172/JCI200318535

Lu Z, Rong K, Li J, Yang H, Chen R (2013) Size-dependent antibacterial activities of silver nanoparticles against oral anaerobic pathogenic bacteria. J Mater Sci Mater Med 24:1465–1471

Luo Y, Hossain M, Wang C, Qiao Y, An J, Ma L, Su M (2013) Targeted nanoparticles for enhanced X-ray radiation killing of multidrug-resistant bacteria. Nanoscale 5(2):687–694. https://doi.org/10.1039/c2nr33154c

Marei N, Elwahy AHM, Salah TA, El-Sherif Y, El-Samie EA (2018) Enhanced antibacterial activity of Egyptian local insects' chitosanbased nanoparticles loaded with ciprofloxacin-HCl. Int J Biol Macromol 126:262–272. https://doi.org/10.1016/j.ijbiomac.2018.12.204

Markova Z, Šiškova K, Filip J et al (2012) Chitosan-based synthesis of magnetically-driven nanocomposites with biogenic magnetite core, controlled silver size, and high antimicrobial activity. Green Chem 14:2550–2558. https://doi.org/10.1039/C2GC35545K

Massart R (1981) Preparation of aqueous magnetic liquids in alkaline and acidic media. IEEE Trans Magn 17(2):1247–1248

McKenzie C (2011) Antibiotic dosing in critical illness. J Antimicrob Chemother 66(Suppl 2):ii25–ii31. https://doi.org/10.1093/jac/dkq516

McQuillan JS, Shaw AM (2014) Differential gene regulation in the Ag nanoparticle and Ag+-induced silver stress response in *Escherichia coli*: a full transcriptomic profile. Nanotoxicology. 8:177–184

Meghana S, Kabra P, Chakraborty S, Padmavathy N (2015) Understanding the pathway of antibacterial activity of copper oxide nanoparticles. RSC Adv 5:12293–12299

Michalikova L, Hnilicova S. and Brnova J (2017) Nanoshield surface coating protection combination with cleaning product cleaner for removal bacterial contamination. Abstracts from the 4th International Conference on Prevention & Infection Control (ICPIC 2017). Geneva, Switzerland. 20–23 June 2017 Antimicrobial Resistance and Infection Control, 6(Suppl 3):P390. https://doi.org/10.1186/s13756-017-0201-4

Mosmann T (1983) Rapid colorimetric assay for cellular growth and survival: application to proliferation and cytotoxicity assays. J Immunol Methods 65:55–63

Muller RH, Jacobs C, Kayser O (2001) Nanosuspensions as particulate drug formulations in therapy. Rationale for development and what we can expect for the future. Adv Drug Deliv Rev 47:3–19

Nair LS, Laurencin CT (2008) Nanofibers and nanoparticles for orthopaedic surgery applications. J Bone Jt Surg Am 90:128–131

Naz et al (2013) Enhanced biocidal activity of Au nanoparticles synthesized in one pot using 2, 4-dihydroxybenzene carbodithioic acid as a reducing and stabilizing agent. J Nanobiotechnol 11:13. https://doi.org/10.1186/1477-3155-11-13

Neu HC (1992) The crisis in antibiotic resistance. Science 257:1064–1073

Niemirowicz et al (2015) Bactericidal activity and biocompatibility of ceragenin-coated magnetic nanoparticles. J Nanobiotechnol 13:32. https://doi.org/10.1186/s12951-015-0093-5

Nordmann P, Poirel L, Walsh TR, Livermore DM (2011) The emerging NDM carbapenemases. Trends Microbiol 19:588–595

Nordmann P, Dortet L, Poirel L (2012) Carbapenem resistance in Enterobacteriaceae: here is the storm! Trends Mol Med 18(5):263–272

Novais Â et al (2012) Spread of an OmpK36-modified ST15 Klebsiella pneumoniae variant during an outbreak involving multiple carbapenem-resistant Enterobacteriaceae species and clones. Eur J Clin Microbiol Infect Dis 31:3057–3063

Omolo CA, Kalhapure RS, Jadhav M, Rambharose S, Mocktar C, Ndesendo VMK, Govender T (2017) Pegylated oleic acid: a promising amphiphilic polymer for nano-antibiotic delivery. Eur J Pharm Biopharm 112:96–108. https://doi.org/10.1016/j.ejpb.2016.11.022

Padmavathy N, Vijayaraghavan R (2008) Enhanced bioactivity of ZnO nanoparticles an antimicrobial study. Sci Technol Adv Mater 9:35004

Palanisamy et al (2014) Antibiofilm properties of chemically synthesized silver nanoparticles found against *Pseudomonas aeruginosa*. J Nanobiotechnol 12:2. https://doi.org/10.1186/1477-3155-12-2

Panáček A, Smékalová M, Kilianová M, Prucek R, Bogdanová K, Večeřová R, Kolář M, Havrdová M, Płaza GA, Chojniak J, Zbořil R, Kvítek L (2015) Strong and nonspecific synergistic antibacterial efficiency of antibiotics combined with silver nanoparticles at very low concentrations showing no cytotoxic effect. Molecules. 21(1):E26

Panáček A, Kvítek L, Smékalová M, Večeřová R, Kolář M, Röderová M, Dyčka F, Šebela M, Prucek R, Tomanec O, Zbořil R (2017) Bacterial resistance to silver nanoparticles and how to overcome it. Nat Nanotechnol 13(1):65–71. https://doi.org/10.1038/s41565-017-0013-y

Park et al (2018) Proteomic analysis of antimicrobial effects of pegylated silver coated carbon nanotubes in *Salmonella enterica* serovar Typhimurium. J Nanobiotechnol 16:31. https://doi.org/10.1186/s12951-018-0355-0

Perez F, Hujer AM, Hujer KM, Decker BK, Rather PN, Bonomo RA (2007) Global challenge of multidrug-resistant *Acinetobacter baumannii*. *Antimicrob*. Agents Chemother 51:3471–3484

Pérez-Díaz MA, Boegli L, James G, Velasquillo C, Sánchez-Sánchez R, Martínez-Martínez R-E, Martínez-Castañón GA, Martinez-Gutierrez F (2015) Silver nanoparticles with antimicrobial activities against *Streptococcus mutans* and their cytotoxic effect. Mater Sci Eng C 55:360–366

Pfeifer Y, Schlatterer K, Engelmann E, Schiller RA, Frangenberg HR, Stiewe D et al (2012) Emergence of OXA-48 type carbapenemase producing Enterobacteriaceae in German hospitals. Antimicrob Agents Chemother 56:2125–2128

Pini A, Giuliani A, Falciani C et al (2005) Antimicrobial activity of novel dendrimeric peptides obtained by phage display